Nuclear Engineering and Design 444 (2025) 114437

Contents lists available at ScienceDirect

Nuclear Engineering and Design

journal homepage: www.elsevier.com/locate/nucengdes

CATHARE calculation of the tests conducted on the ELSMOR passive heat removal system

B. Grosjean [a,*], R. Ferri [b], C. Lombardo [c]

[a] CEA Cadarache, DES/IRESNE/DER, 13108 Saint-Paul-lez-Durance, France
[b] SIET, Via Nino Bixio 27/c, 29121 Piacenza, Italy
[c] ENEA, NUC-ENER-SIC, Via dei Mille 21, Bologna, Italy

ARTICLE INFO

Keywords:
DHR
ELSMOR
Natural circulation
Passive system
CATHARE
CSG

ABSTRACT

As part of the ELSMOR (Toward European Licensing of Small Modular Reactors) project, an experimental facility has been set up at SIET (Piacenza, Italy) to test a passive heat removal system. Such a passive system operates in natural circulation, with three different circuits: a primary circuit (PC, the heat source), a secondary circuit (SC, self-pressurised) and a tertiary circuit (the heat sink, represented by a pool). The primary and the secondary circuits are thermally coupled to a plate-type Compact Steam Generator (CSG), while the secondary and the tertiary circuits are coupled to an in-pool condenser. An experimental campaign has been carried out to investigate the effect of different parameters on the passive system behavior, through different types of tests (e.g. secondary side filling ratio (FR) or non-condensable gas (NC) concentration, primary system temperature, pool level, etc.). These experimental tests are modelled with the CATHARE 3 code (French system calculation code) and the calculation results are compared with the experimental data. The CATHARE 3 code predicts good tendencies for the tests on the main parameters of the facility (exchanged power, secondary circuit pressure, condenser outlet temperature). For the majority of the tests, the discrepancy between experimental and calculation results for the exchanged power in the CSG is below 10 %: for high FR in the SC, the CATHARE 3 code predicts the exchanged power well, while for low FR the power is overestimated. Sensitivity calculations showed that the condenser has the main influence on the facility behavior (the CSG has a limited influence); in particular, the correlations in the secondary side of the condenser have a significant influence on the exchanged power, while the correlations in the tertiary side have a small influence; thus, the tertiary modelling has a small influence on the calculation results. For all tests, the CATHARE 3 code underestimates the SACO outlet temperature and overestimates the pressure in the SC. Nonetheless, the presence of experimental uncertainties, particularly related to uncharacterized head losses and two-phase flow conditions, prevents drawing fully conclusive statements about the model accuracy.

1. Introduction

In recent years, Small Modular Reactors (SMR) have attracted growing interest as a means to provide flexible, low-carbon energy with enhanced safety features. These reactors are designed with simplified architectures, lower power outputs, and rely heavily on passive safety systems to respond to design-basis and beyond-design-basis accidents. In parallel, nuclear regulatory authorities are increasingly emphasizing the need for robust experimental validation to support the licensing of such innovative systems. However, current experimental databases and validation frameworks are primarily oriented toward large-scale Pressurized Water Reactors, leaving a gap in the assessment of SMR-specific technologies. This work contributes to bridging that gap by addressing one of the key components of SMR passive safety architectures: the residual heat removal system based on a Safety Condenser and Compact Steam Generator.

Passive safety systems operate based on fundamental physical mechanisms – such as gravity, pressure gradients, and natural convection – allowing them to perform critical safety functions without relying on external power sources. In nuclear reactors, these systems play a vital role in tasks like removing residual core heat, replenishing coolant inventory in the primary circuit, or cooling the containment structures (International Atomic Energy Agency, 2020; NEA-OECD, 2024). Among these, a notable example is the passively cooled Steam Generator (SG), also known as the Safety Condenser (SACO). This system enables the

* Corresponding author.
E-mail address: baptiste.grosjean@cea.fr (B. Grosjean).

https://doi.org/10.1016/j.nucengdes.2025.114437
Received 12 May 2025; Received in revised form 29 July 2025; Accepted 30 August 2025
Available online 1 September 2025

Nomenclature

Abbreviations

CATHARE	Code for Analysis of THermalhydraulics during an Accident of Reactor and safety Evaluation
CL	Cold leg
CSG	Compact Steam Generator
ELSMOR	Towards European Licencing of Small Modular Reactors
FR	Filling Ratio
HL	Hot leg
HX	Heat exchanger
MF	Mass fraction
NC	Non-condensable
PC	Primary circuit
PS	Primary side
SACO	SAfety COndenser
SC	Secondary circuit
SG	Steam Generator
SMR	Small Modular Reactor
SS	Secondary side

Notations

α	Void fraction
C_p	Heat capacity ($J.kg^{-1}.K^{-1}$)
L	Latent heat ($J.kg^{-1}$)
m	Mass (kg)
Nu	Nusselt number
Pr	Prandtl number
P_W	Power (W)
Q	Flowrate (kg/s)
Re	Reynolds number
t	Time (s)
T	Temperature (°C)

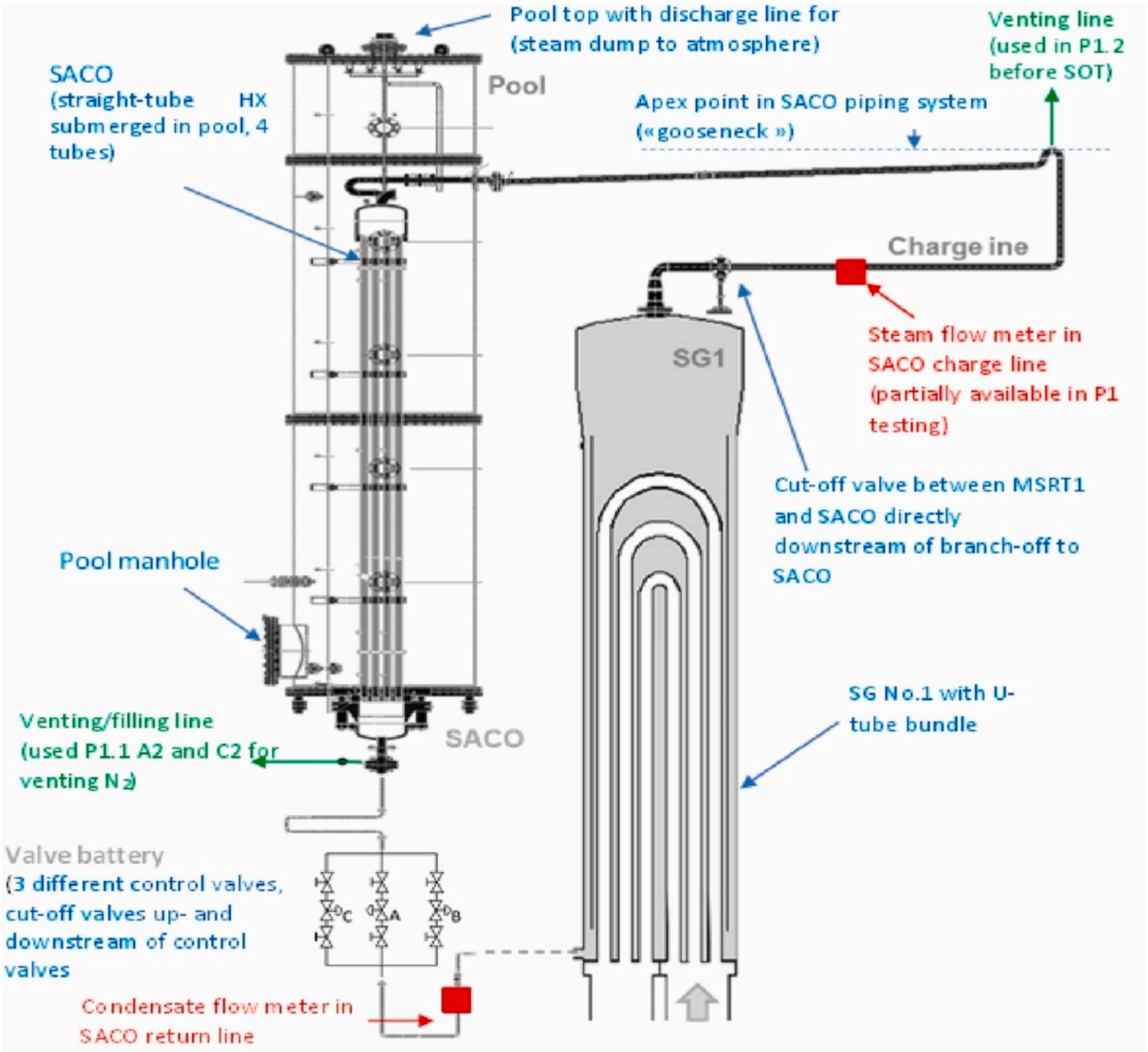

Fig. 1. Schematic diagram of a SACO connected to a SG – PKL facility (Montout et al., 2024).

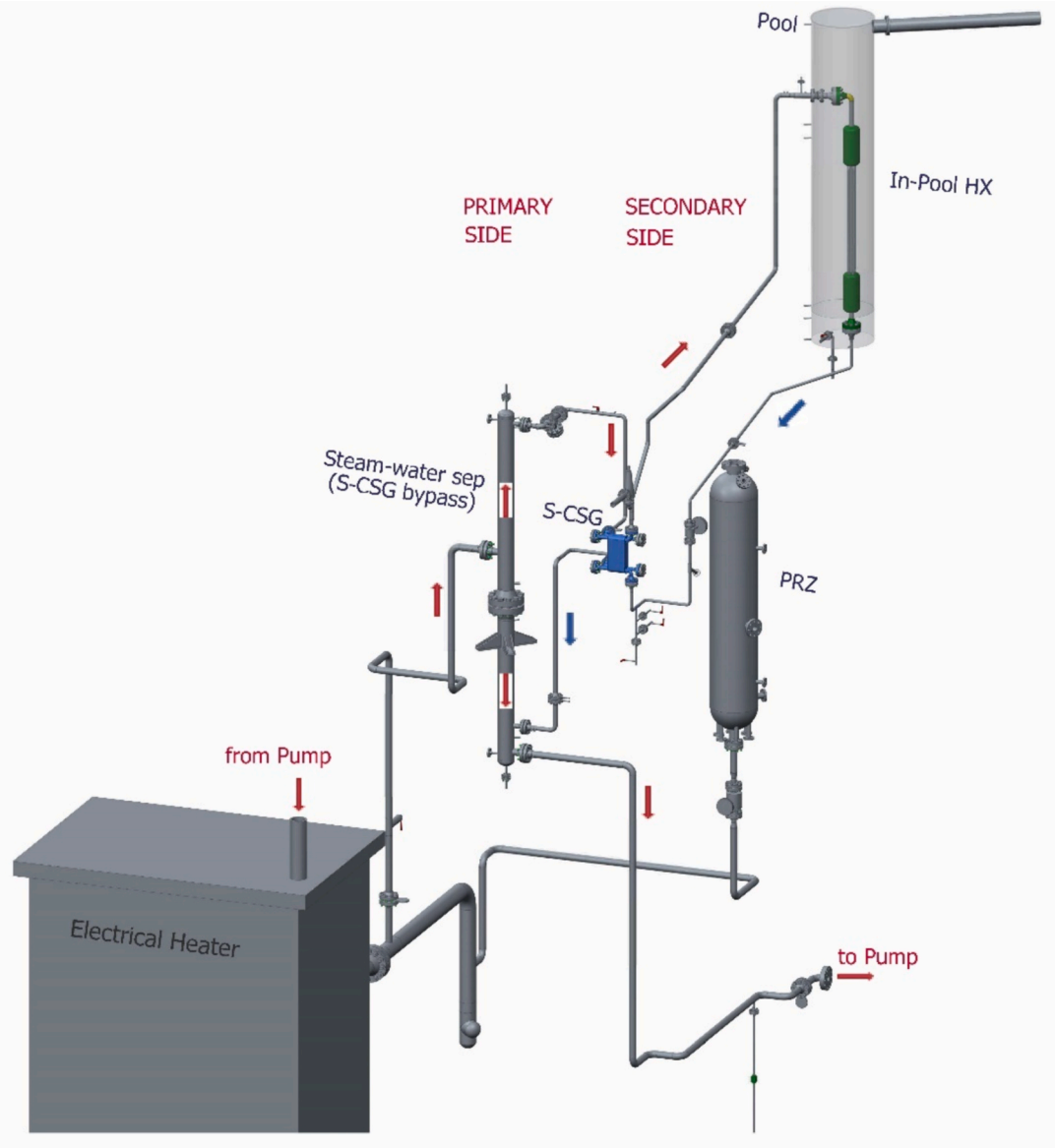

Fig. 2. Overview of ELSMOR facility (Ferri et al., 2023a).

removal of decay heat from the reactor core by passively cooling the secondary side. It functions by condensing steam from the SG in a heat exchanger submerged in a water pool, with the resulting condensate returning to the SG's downcomer through natural circulation. A schematic diagram of a SACO connected to a SG is presented in Fig. 1 (PKL facility, (Montout et al., 2024)). Such passive safety systems have been incorporated into the design of several advanced high-power reactors, including the AES-2006 (Bakhmet'ev et al., 2009), APR+ (Bae et al., 2012), CPR-1000 (Zhang et al., 2012) and HPR-1000 (Xing et al., 2016). The NUWARD Small Modular Reactor (SMR) was also intended to incorporate a passive residual heat removal system featuring a Safety Condenser, as part of its safety architecture (Francis and Beils, 2024). These implementations feature a variety of heat exchanger configurations, ranging from vertical to inclined orientation.

In order to validate the performance of SACO and/or the whole passive residual heat removal systems, as well as to assess the accuracy of thermal–hydraulic simulation tools, several Integral Effect Test facilities have been developed. These experimental setups aim to replicate the key physical phenomena occurring in nuclear power plants under transient or accidental conditions, allowing for both the qualification of system behavior and the benchmarking of computational codes used in safety analysis. The ATLAS facility at KAERI (South Korea) (Bae et al., 2012) was designed and exploited to study the performance of a passive auxiliary feedwater system consisting of a horizontal (slightly inclined) in-pool heat exchanger. The NOKO experiment (Schaffrath et al., 1999) was designed and exploited to simulate the emergency condenser of the SWR-1000 design. The PERSEO (in-Pool Energy Removal System for Emergency Operation) test facility at the SIET laboratories in Piacenza, Italy, investigated the operational principles of a decay heat removal system utilizing a vertical pool heat exchanger (Achilli et al., 2002). In the frame of the PASTELS European project, a SACO was implemented at the secondary side of the PKL facility and studied to expand the experimental knowledge on the steady and transient performance of this component (Gómez-García-Toraño et al., 2025).

Despite the valuable insights gained from these Integral-Effect Tests, they generally do not encompass the full system-level behavior of passive residual heat removal architectures. Many of the aforementioned experiments isolate the SACO and provide it with predefined thermal–hydraulic boundary conditions, rather than embedding it within a fully integrated loop that reflects realistic reactor configurations. As a result, key interactions between the SACO, the primary and secondary systems, and other components are not adequately captured. Moreover, none of

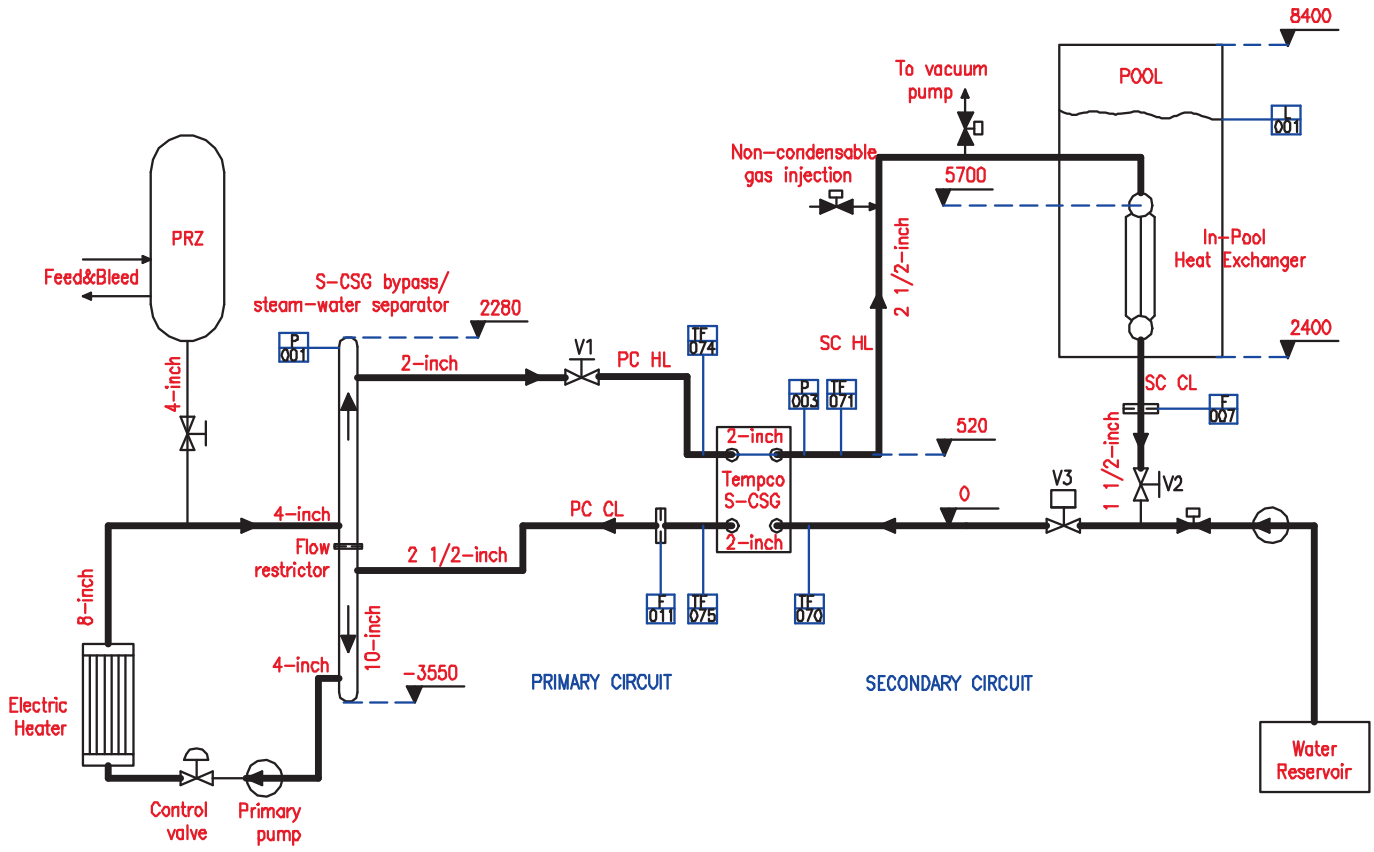

Fig. 3. Overview of ELSMOR facility (Ferri et al., 2023b).

the existing test facilities incorporate a plate-type Compact Steam Generator (CSG), as foreseen in the NUWARD design. This type of steam generator exhibits thermal–hydraulic behavior that differs significantly from traditional U-tube or once-through steam generators, particularly in terms of heat transfer characteristics, flow distribution, and dynamic response during transients. Therefore, current experimental setups are not fully suitable for validating the passive residual heat removal system envisioned for NUWARD, especially under representative operational and accidental conditions involving CSG-specific phenomena.

To address these validation gaps and to support the safety demonstration of SMR-specific configurations such as NUWARD, the ELSMOR project was initiated.

The ELSMOR project addresses some critical aspects of Light Water (LW) Small Modular Reactor (SMR) licensing, as a response to the Horizon 2020 Euratom NFRP-2018-3 call entitled “Research on the safety of Light Water Small Modular Reactors”. The project establishes a thorough assessment methodology for such purposes, based on extensive experimental and analytical work. In addition, the project provides a platform for a more active dialogue between regulators and industry representatives to accelerate the deployment of LW-SMRs in Europe. The consortium brings together 15 partners from 8 European countries, including research institutes, major European nuclear companies and technical support organisations. The project was launched in September 2019, with a planned duration of 3.5 years (extended to 4 years). Thanks to the results of the ELSMOR project, the licensing process for LW-SMRs can be streamlined and optimised, allowing early deployment.

However, as highlighted previously, the validation of passive residual heat removal systems specifically designed for SMRs like NUWARD still presents notable gaps – particularly regarding systems involving CSGs, which are absent from existing integral-effect facilities. The ELSMOR project directly addresses this limitation by proposing a test configuration that incorporates such a component, thereby offering a more representative environment for evaluating CSG-integrated passive safety systems.

In this scope, within the ELSMOR project, a single experimental facility – which shares the same name as the project – has been designed and built at SIET (Piacenza, Italy). The aim of the facility is to study a passive heat removal system operating in natural circulation. The facility includes three different circuits: a primary circuit (the heat source), a secondary circuit (self-pressurised) and a tertiary circuit (the heat sink, represented by a pool). The primary and the secondary circuits are thermally coupled to a plate-type CSG, while the secondary and the tertiary circuits are coupled to an in-pool condenser. The condenser is a bundle of five vertical straight tubes immersed in the pool. This configuration allows for the investigation of the coupled dynamics between a plate-type steam generator and a SACO, under thermally and hydraulically realistic conditions that are closer to those expected in a NUWARD-like reactor. In order to better understand the behavior of such a two-phase natural circulation heat removal loop, an experimental campaign has been carried out on this facility. The effect of different parameters on the passive system behavior has been investigated through different types of tests (e.g. secondary side filling ratio or non-condensable concentration, primary system temperature, pool level, etc.) to address the main expected physical phenomena (balance between the driving force (density difference) and pressure losses in natural convection, nucleate boiling in the CSG, steam condensation and nucleate boiling in the condenser; two-phase flow in the secondary circuit and in the pool).

A benchmark between European reference codes (Apros, AC^2, CATHARE, RELAP5 and TRACE) has been carried out (Bersano et al., 2024), on a specific test (ELSMOR test 00099_C). All the codes were able to reproduce the experimental data both qualitatively and quantitatively. However, some discrepancies were observed in the calculated results, particularly regarding the prediction of the secondary side

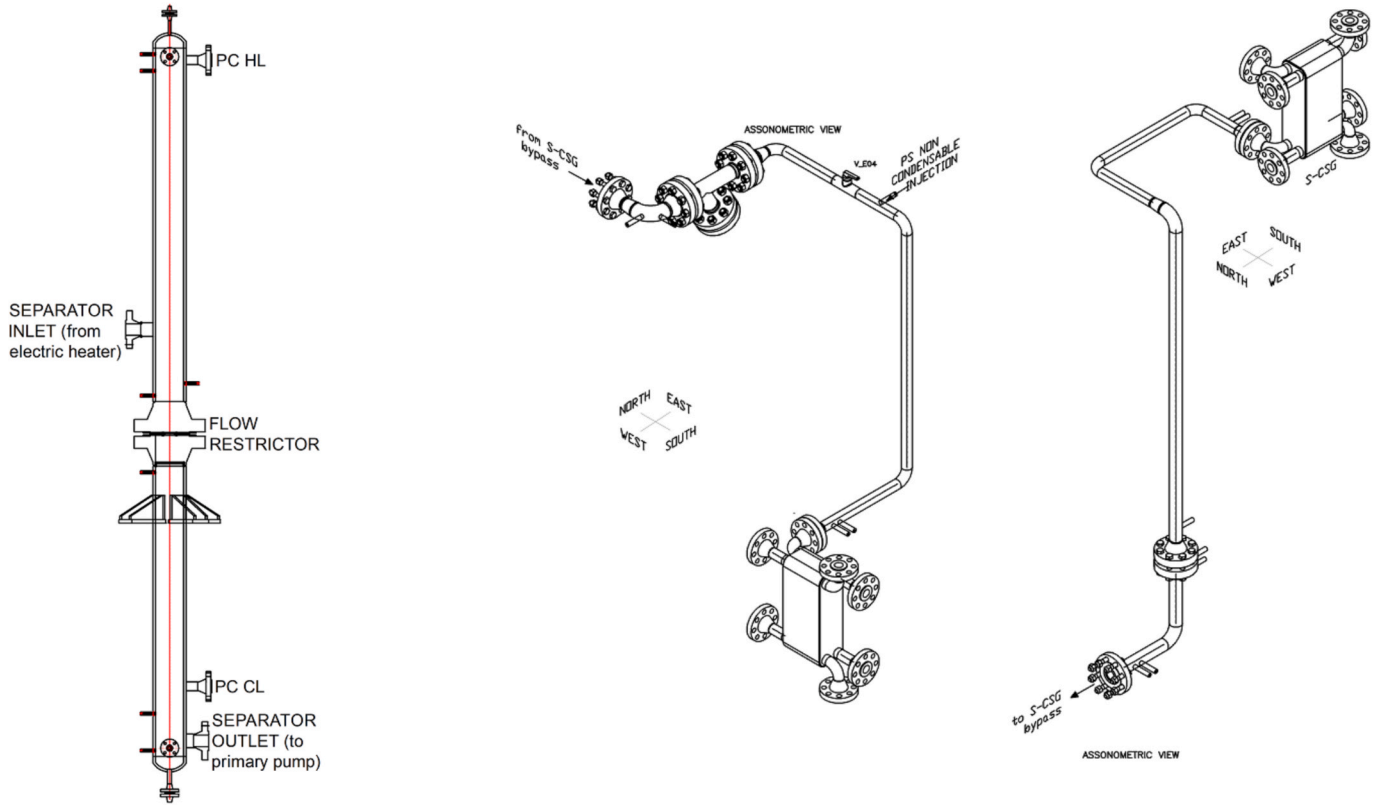

Fig. 4. S-CSG bypass/steam-water separator (left); PC Hot leg (center); PC Cold leg (right).

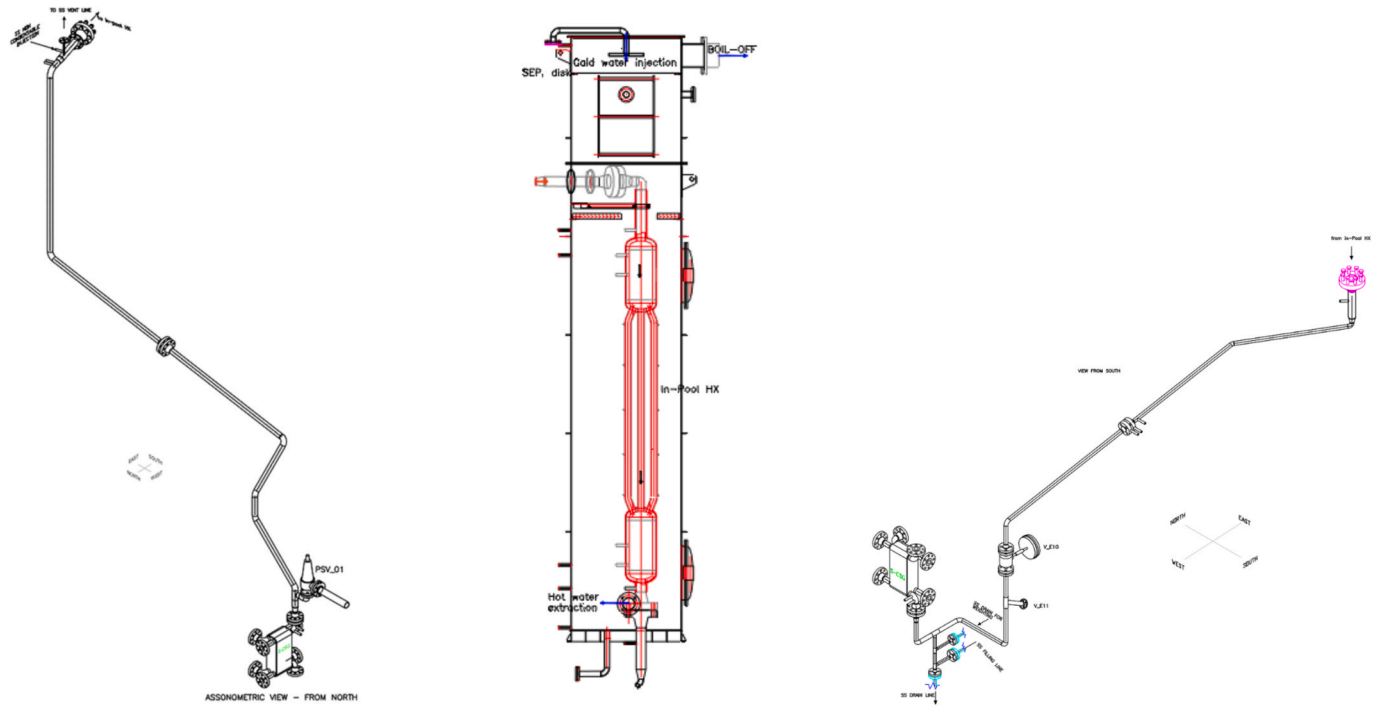

Fig. 5. SC Hot leg (left); In-Pool heat exchanger (center); SC Cold leg (right).

pressure, the CSG inlet temperature on the secondary side, and the secondary side flow rate. The present work represents the continuation of this work with new CATHARE 3 calculations performed at CEA: sensitivity calculations were performed on the test used for the ELSMOR benchmark (to investigate the discrepancies with the experimental results) and additional calculations (also including sensitivity calculations) were also carried out on two other tests of the experimental campaign.

A brief description of the ELSMOR facility is given in section 2, presenting the main components and circuits of the loop. The test matrix

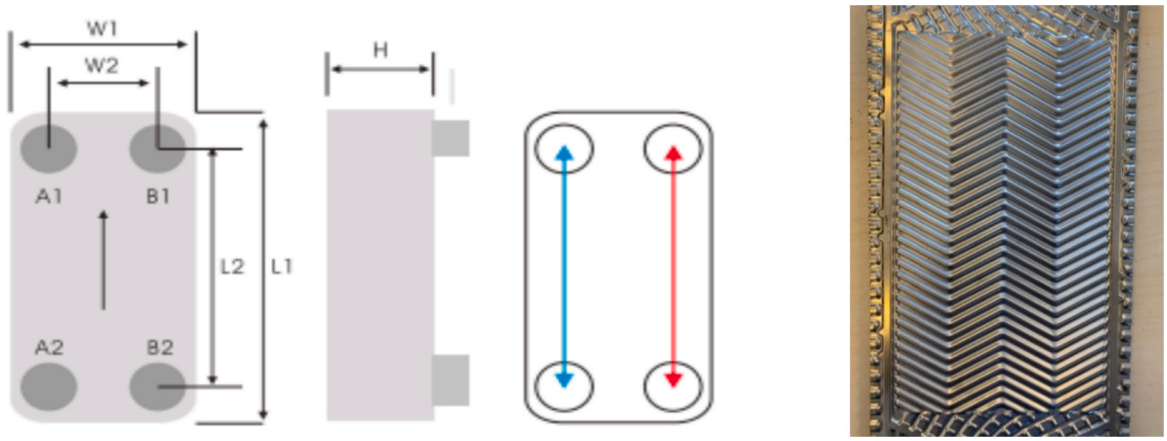

Fig. 6. Diagram of the CSG (left); View of a plate (right).

Table 1
Characteristics of the CSG.

Parameter	Dimension (see Fig. 6)	Value	Unit
Plate number	N	130	
Total height	L1	0.616	m
Longitudinal nozzle distance	L2	0.519	m
Total width	W1	0.189	m
Transversal nozzle distance	W2	0.092	m
Thickness	H	0.2935	m
Weight		110.56	kg
Heat transfer area/plate		0.095	m^2
Total heat transfer area		12.16	m^2
Volume/channel		0.000156	m^3
Total volume		0.020124	m^3

Table 2
Tests performed on ELSMOR facility.

Group	Purpose of investigation
A	Investigate the behavior of the plant in the presence of a fix quantity of non-condensable gas in the SC since the beginning of the transient (288.13 Nl of air), at constant FR (20 %), at different primary side temperatures (260 to 320 °C) and at reduced HX-Pool level (last part of the test).
B	Investigate the behavior of the plant without non-condensable gas in the SC, at decreasing FR (15.2 to 11.9 %) down to circulation destabilization, at increasing FR (15.9 to 16.32 %) up to re-stabilization, at decreasing FR (16.32 to 14.39 %) down to destabilization, at constant PC temperature (320 °C), at high level in the HX-Pool.
C	Investigate the behavior of the plant with the valve V_E04 on the primary side partialized, with increasing quantity of non-condensable gas in the SC (0 to 1402.21 Nl of N_2) at constant FR (31.20 %) and at constant PC temperature (320 °C). Once reached the maximum quantity of injected non-condensable gas, it explores decreasing FR (31.20 to 20.40 %).
D	Investigate the behavior of the plant with the valve V_E04 on the primary side partialized, without non-condensable gas in the SC, at decreasing FR (60.16 to 14.08 %) down to circulation destabilization, at increasing FR (14.08 to 18.16 %) up to re-stabilization, at constant high PC temperature (310 °C). Once circulation is re-stabilized and FR increased up to 30 %, it explores the plant behavior at decreasing FR (30 to 15.44 %) down to circulation destabilization, at increasing FR (15.44 to 16.91 %) up to re-stabilization, at constant low PC temperature (260 °C).
E	Investigate the behavior of the plant with the valve V_E04 on the primary side and the valve V_E11 on the secondary side partialized (V_E11 10/12 turn open), without non-condensable gas in the SC, at decreasing FR (30.64 to 14.34 %) down to circulation destabilization, at increasing FR (14.34 to 16.17 %) up to re-stabilization, at constant PC temperature (310 °C). Once circulation is re-stabilized and FR increased up to 30.65 %, it explores the plant behavior at increasing closure of the valve V_E11 (10/12 turn open to complete closure) and back to initial position (10/12 turn open) with circulation destabilization and stop up to circulation re-stabilization, at constant FR (30.65 %), at constant PC temperature (310 °C).
F	Investigate the behavior of the plant with the primary side in two-phase conditions, i.e. with low level in the Separator and steam in condensation in the CSG primary side, without non-condensable gas in the SC, at decreasing FR (39.2 to 20 %) and at constant PC temperature (310 °C).
G	Investigate the behavior of the plant without non-condensable gas in the SC, at decreasing FR (32.08 to 21.07), at different primary side temperatures (250 to 310 °C) and at reduced HX-Pool level (last part of the test).

is described in section 3, where the seven groups of tests are detailed along with the investigated parameters and their objectives. The nodalisation developed for the CATHARE 3 code and used for the calculations is described in section 4. In section 5, for each of the three simulated tests, the CATHARE results – including both best-estimate and sensitivity calculations – are compared to the experimental data. Finally, the main conclusions are summarised in section 6.

2. ELSMOR facility

Fig. 2 and Fig. 3 shows the layout of the ELSMOR facility constructed at SIET (Ferri et al., 2023a,b). The ELSMOR facility mainly consists of three circuits, thermally coupled by a plate-type CSG and a condenser:

- The Primary Circuit (PC), mainly operating with single-phase liquid water in forced circulation, can also operate in two-phase conditions with the primary system in saturation (low steam quality) at the outlet of the electric heater: steam and water are subsequently separated in the separator with steam flowing to the CSG and water being returned to the electric heater. With reference to Fig. 3, the part of interest of the PC includes the S-CSG bypass/steam-water separator and the pipes to the S-CSG which layout is reported in Fig. 4, the rest of the loop is considered as a supply system of fluid at the required conditions.
- The Secondary Circuit (SC) operates in natural two-phase circulation. The heat provided in the CSG (heat source) drives the natural circulation in the SC. The SC is self-pressurised, and the pressure depends on the FR and the thermohydraulic conditions on both the primary and tertiary sides. The piping layout and the in-Pool heat exchanger are reported in Fig. 5.
- The Tertiary Circuit (TC), which is the pool (heat sink of the SC through the submerged vertical tube bundle Heat eXchanger (HX) also called condenser) operates in natural circulation. The HX in the pool is represented in Fig. 5.

The power/volume scaling factor of the facility is approximately 1:50 and the height factor is 1:1 (Ferri et al., 2023a). The main components of the facility, presented in Fig. 2 to Fig. 5, are (Ferri et al., 2023a):

Table 3
Estimated measurement uncertainties for the main ELSMOR data (Ferri et al., 2023a).

Quantity	Variable	Units	Measure	Expanded uncertainty	U (%)
Primary side pressure	P_001	MPa	11.92	0.01	0.1
Secondary side pressure	P_003	MPa	6.45	0.01	0.2
CSG primary side inlet temperature	TF_074	°C	310.9	0.15	0.0
CSG primary side outlet temperature	TF_075	°C	281.7	0.15	0.1
CSG secondary side inlet temperature	TF_070	°C	266.3	0.15	0.1
CSG secondary side outlet temperature	TF_071	°C	280.3	0.15	0.1
Pool water level	L_001	m	4.01	0.06	1.4
CSG primary side flow rate	F_011	kg/s	3.576	0.171	4.8
CSG secondary side flow rate	F_007	kg/s	0.555	0.007	1.3
PC CSG power	W_CSG	kW	575	30	5.2
Filling Ratio	FR	–	30	0.06	0.2

Note 1: Fig. 3 shows the position of the measurement points in the loop. The CSG Power and the Filling Ratio are derived quantity and they are not indicated as measurement points.
Note 2: Expanded uncertainty represents the 95 % probability that a measure falls in the interval "Measure ± Exp. Unc." and it includes the complete measurement chain from the sensor, to the DAS board, to all uncertainties entering the derivation formulas.
Note 3: U% represents the percentage uncertainty referred to the measurement.

- An electric heater, providing the primary system with water or steam at the CSG, with the desired inlet conditions;
- The S-CSG bypass (or steam-water separator), which receives the hot fluid from the electric heater, delivers a certain flow rate to the primary side of the CSG and recirculates the remaining portion to the outlet of the separator. An orifice plate in the separator allows the desired flow distribution in the primary system to be achieved in subcooled liquid tests;
- The PC Hot Leg (HL), which connects the separator top outlet nozzle to the CSG primary inlet nozzle;
- The CSG, which is an HX plate-type with 130 plates;
- The PC Cold Leg (CL) connecting the CSG outlet nozzle to the separator;
- The SC hot leg, which connects the secondary side CSG outlet nozzle to the In-Pool HX inlet;
- The In-Pool HX (also known as SAfety COndenser or SACO), which is a bundle of five vertical tubes, approximately 2 m long, with two cylindrical headers;
- The Secondary Side Cold Leg, which connects the In-Pool HX outlet to the CSG secondary side inlet nozzle;
- The pool containing the In-Pool HX, approximately 1 m in diameter and 5.5 m in height, with a boil-off pipe;
- Auxiliary piping and components, e.g. for charging and discharging the water in the PC, SC and the pool, for injecting non-condensable gases if required, for circulating the PC water, etc.

Fig. 3 reports the elevations of the main components and the size of the main pipes. Pressure drops along the loop are mainly due to friction and geometrical discontinuities on pipes. The most interesting component is the S-CSG and its pressure drops were measured during ELSMOR tests, in particular for liquid single phase on the primary circuit, 12.2 MPa pressure, 320 °C temperature and 3.4 kg/s flowrate, pressure drops were around 20 kPa while for two-phase on the secondary circuit, 7 MPa pressure, 282 °C temperature and 0.38 kg/s flowrate, pressure drops were around 5 kPa (Ferri et al., 2023b).

A diagram of the CSG, along with a view of a plate, is presented in Fig. 6. Table 1 provides the characteristics of the CSG.

The geometric characteristics of the facility are summarised in (Bersano and Lombardo, 2022; Ferri et al., 2023a,b). The facility is mainly constructed of stainless steel. Insulation is used to reduce the heat losses from the main components and pipework and the pool is also insulated. The instrumentation and data acquisition system of the facility is described in (Ferri et al., 2023a,b).

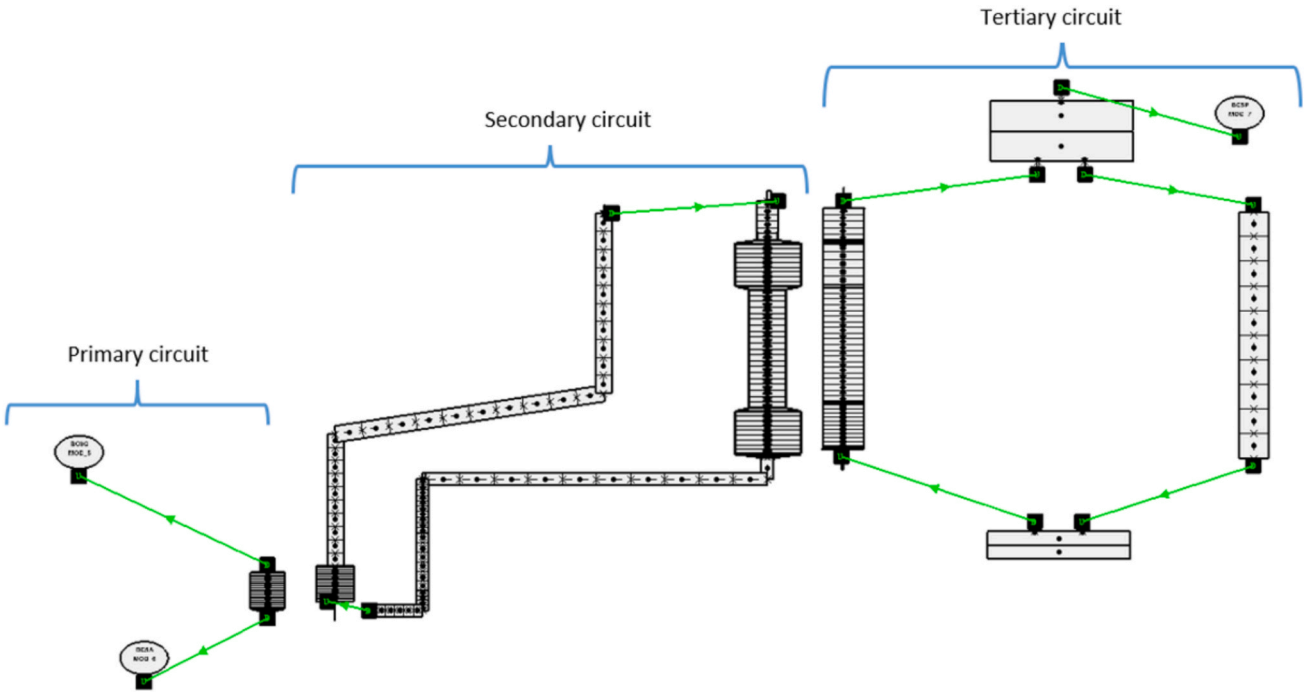

Fig. 7. ELSMOR facility CATHARE nodalization.

Table 4
ELSMOR_00099_C tests and events timing.

Time (s)	Event	Notes
0	Initial filling ratio of the secondary side: 60.16 %Vacuum in the SS: 0.5 bar.	Valve V_E04 7 turns open out of 9.5 turns
73	Triggering valve V_E10 opened	Start-up (Triggering valve opening). Vacuum conditions in the SS.
74–299	Natural circulation start-up and stabilization	
360–660	**Steady state at PS T (TF_082) 309.6 °C; FR 60.16 %**	
700–1140	PS temperature stabilization around 310 °C	
978–1060	6.5 kg mass extracted from the SS; FR 55.04 %	
1140–1440	**Steady state at PS T 310.8 °C; FR 55.04 %**	
1550–1625	6.28 kg mass extracted from the SS; FR 50.00 %	
1900–2300	**Steady state at PS T 310.0 °C; FR 50.00 %**	
2860–2930	6.22 kg mass extracted from the SS; FR 45.04 %	
3070–3600	**Steady state at PS T 309.8 °C; FR 45.04 %**	
3615–3708	6.30 kg mass extracted from the SS; FR 40.00 %	
3890–4350	**Steady state at PS T 309.7 °C; FR 40.00 %**	
4390–4470	6.35 kg mass extracted from the SS; FR 34.92 %	
4500–4900	**Steady state at PS T 310.0 °C; FR 34.92 %**	
5349–5502	6.05 kg mass extracted from the SS; FR 30.08 %	
5630–6400	**Steady state at PS T 309.9 °C; FR 30.08 %**	
6506–6600	6.4 kg mass extracted from the SS; FR 24.96 %	
6700–7000	**Steady state at PS T 309.9 °C; FR 24.96 %**	
7075	Refilling of HX-Pool from the bottom	
7275–7353	**6.3 kg mass extracted from the SS; FR 19.92 %**	

Table 5
Experimental and calculation initial values of the test ELSMOR_00099_C for the main loop parameters.

Parameter	Experimental initial value	CATHARE initial value
Primary-side CSG inlet temperature	310.1 °C	310 °C
Primary-side CSG inlet flowrate	3.47 kg/s	3.5 kg/s
Primary-side CSG inlet quality	0	0
SC filling ratio	60.16 %	60.1 %
SC non-condensable mass	Supposed 0 g	0 g
Pool temperature	10.9 °C	10 °C

3. Experimental campaign

The experimental test matrix was designed on the basis of pre-test calculations carried out by ENEA using the RELAP5 code (Bersano and Lombardo, 2022) which helped to finalize the design of the facility. The test matrix performed by SIET consisted of a total of 81 tests, divided into 7 groups. Table 2 shows the subdivision in groups and provides a brief description of the purpose of investigation for each group. All experimental tests were conducted during the ELSMOR project. The test from Group D was used as the benchmark within the ELSMOR project.

The description of the test procedure, the instrumentation and the experimental test results are given in (Ferri et al., 2023a,b). The main objective of the tests was to investigate different steady state conditions to analyse the effect of different parameters (e.g. primary pressure and temperature, secondary FR, amount of non-condensable gases, etc.) on the system behavior. In addition, the transients between steady state operating conditions, within a group of tests, were also recorded during the experiments.

The detailed description of the test from Group D (used as the benchmark in the ELSMOR project and for which new calculations have been carried out in the present work), as well as of the newly simulated tests from Groups C and F, is provided in the corresponding sections of Chapter 5.

Table 3 shows the estimated measurement uncertainties for the main ELSMOR data.

4. ELSMOR facility nodalisations with the CATHARE code

The nodalisation is developed for CATHARE 3 v2.3.0 code (Préa et al., 2020) and is based on the geometric description of the SIET loop provided by the ELSMOR partners. The components of the facility are represented by Volumes (0D-elements), Pipes (1D-AXIAL-elements), Junctions and Valves. Initial and boundary conditions are imposed using the MODELMOD directive, which allows constant values of reference parameters to be maintained at boundary conditions.

The nodalisation, shown in Fig. 7, consists of:

- A simplified primary circuit showing only the CSG primary side. This part is modelled with a single 1D-Axial-Element: its dimensions and exchange surface are in accordance with the specifications provided by the CSG manufacturer (see Table 1). Mass flow and temperature are imposed at the inlet while pressure is imposed at the outlet.
- The secondary circuit, which includes the HX tubes in the pool, the CSG secondary side, the secondary hot leg and the cold leg. All of these elements are modelled by 1D-Axial-Elements. More specifically, one AXIAL element represents the CSG and the hot leg while another AXIAL element represents the condenser and the cold leg. These two AXIAL-elements are connected by 2 Junctions (one at the CSG inlet and another at the HX inlet in the pool) to form a closed loop. The total mass of water contained in this closed loop is regulated by a gadget (called PIQUAGE, which allows the injection or extraction of fluid in the element) in the secondary cold leg in order to obtain the desired secondary filling ratio throughout the transient. A valve is also modelled in the cold leg: it can be used to regulate the secondary flow. The singular pressure losses in the secondary system are implemented for each change of direction, and each increase/decrease in pipe section, using (Idelchik, 2008). A singular pressure loss has also been added to account for the flow resistance due to the CSG, which is estimated from data provided by the manufacturer (this point will be discussed later in the paper). In addition, the primary system is thermally connected to the secondary system by the heat structure simulating the CSG plates.
- The pool with an atmospheric pressure boundary condition in its upper part. Its model contains two AXIAL-elements, respectively the ascending flow near the HX tubes and the descending flow far from the tubes, and two VOLUME-elements representing the upper part of the pool (with atmospheric pressure boundary condition) and the lower part of the pool. A PIQUAGE gadget controls the initial pool level. Finally, the pool is thermally coupled to the secondary circuit through the heat structures with three EXCHANGER modules, simulating the HX headers in the pool, the tube bundle and the piping in the pool.

The modelling of the flow in the pool is based on previous work carried out by CEA on in-pool heat exchangers (Vernassière, 2022). Some sensitivity calculations are performed on this modelling to see the impact on the results (see Chapter 5).

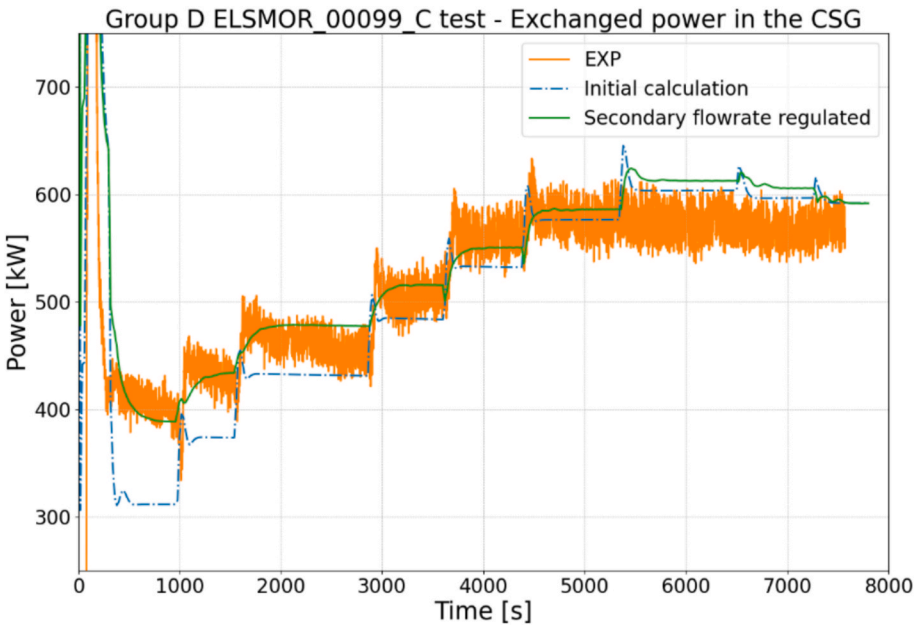

Fig. 8. Group D ELSMOR_00099_C test – Exchanged power in the CSG – Initial calculation and calculation with secondary flow rate controlled, compared to experimental data (EXP).

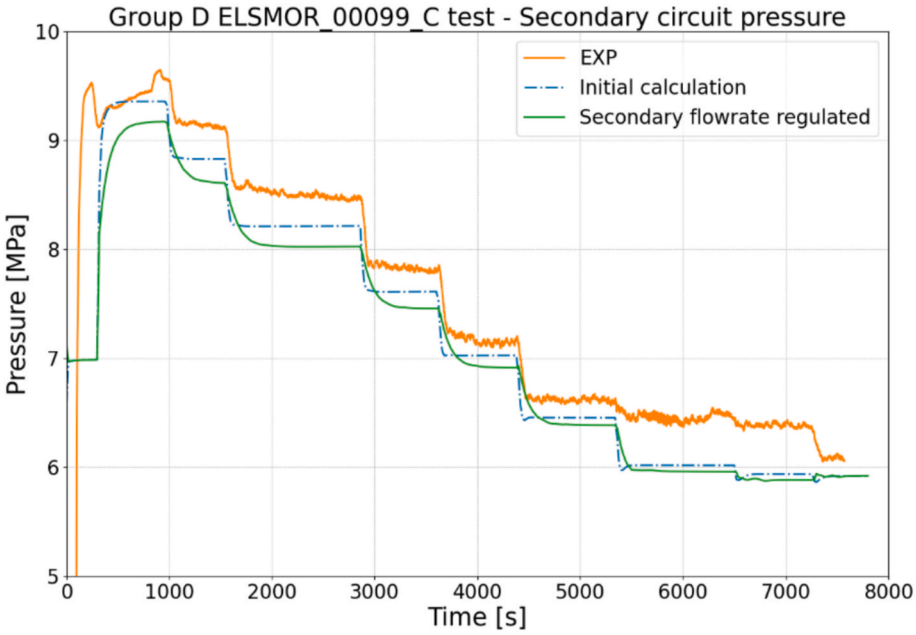

Fig. 9. Group D ELSMOR_00099_C test – Secondary circuit pressure – Initial calculation and calculation with secondary flow rate controlled, compared to experimental data (EXP).

Heat structures are assigned to all pipes in the secondary system in order to model thermal inertia (no heat losses are modelled, they are supposed to be negligible due to the presence of insulating material). Moreover, the modelling of both the CSG and the condenser does not include fouling.

As no characterisation tests have been carried out on the experimental loop, the singular head losses have not been included in the modelling: the implications are discussed in Chapter 5.

5. Calculation results

The calculations were also carried out using version v2.3.0 of the CATHARE 3 code (Préa et al., 2020).

For each experimental group, one steady state test point has been selected and simulated. Among them, three tests have been selected and described in this paper. The description of the test is given in the corresponding section:

- Test ELSMOR_00099_C (from group D), selected for the benchmark carried out during the ELSMOR project (Bersano et al., 2024) and investigating the influence of the FR in the SC on the facility behavior,

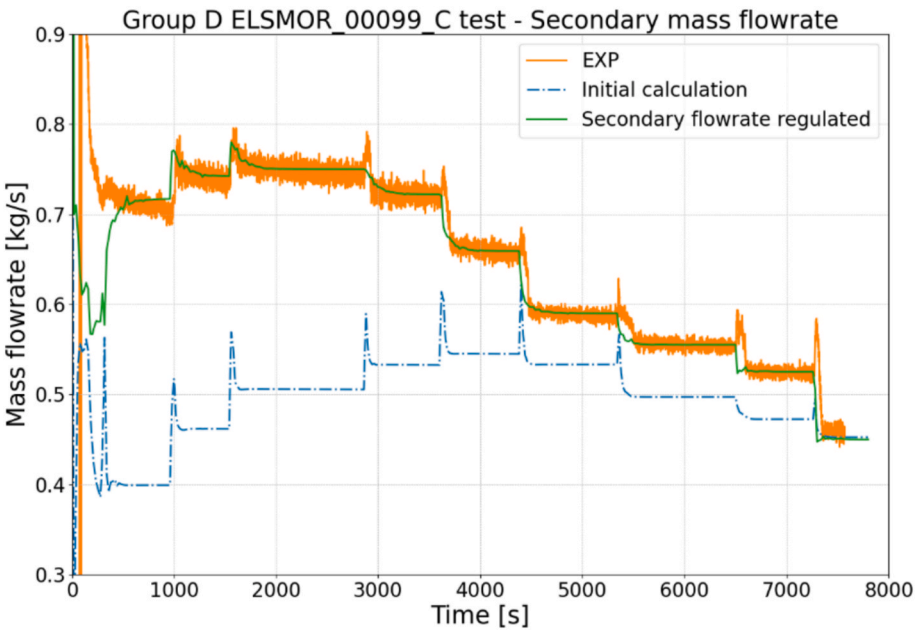

Fig. 10. Group D ELSMOR_00099_C test – Secondary mass flowrate – Initial calculation and calculation with secondary flow rate controlled, compared to experimental data (EXP).

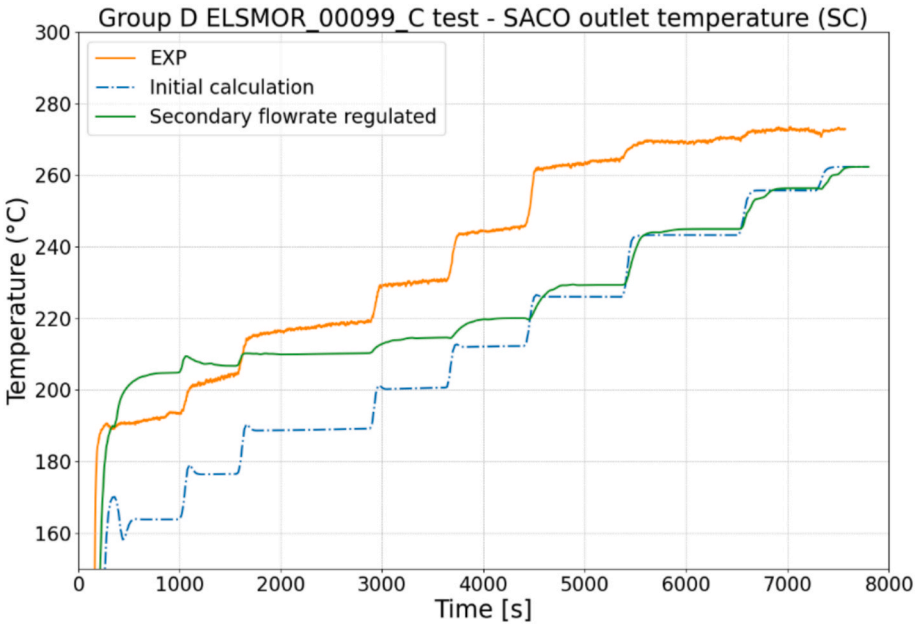

Fig. 11. Group D ELSMOR_00099_C test – SACO outlet temperature (SC) – Initial calculation and calculation with secondary flow rate controlled, compared to experimental data (EXP).

- Test ELSMOR_00090_C_C (from group C), which investigates the impact of the presence of non-condensable gas in the SC on the facility behavior,
- Test ELSMOR_00134_C (from group F), which investigates the behavior of the facility with a two-phase flow on the primary side of the CSG.

The main parameter compared between the CATHARE 3 calculations and the experimental results is the extracted power through the CSG. Some other parameters (e.g. the secondary circuit pressure) are also compared.

5.1. *Test ELSMOR_00099_C – Group D*

The first test presented in this chapter is the one selected for the benchmark carried out during the ELSMOR project (Bersano et al., 2024).

Table 4 shows the timing of events of the ELSMOR_00099_C test. The main objective of this test is to characterise the effect of the secondary circuit liquid mass (from 60 % (high mass) to 20 % (low mass) FR) on the loop performance (i.e. the power extracted from the primary circuit by the steam generator), with fixed primary conditions (liquid water with an inlet temperature of 310 °C and a flow rate of 3.5 kg/s).

To model this test, the boundary conditions are imposed on primary side of the CSG. The secondary circuit liquid mass is controlled (using

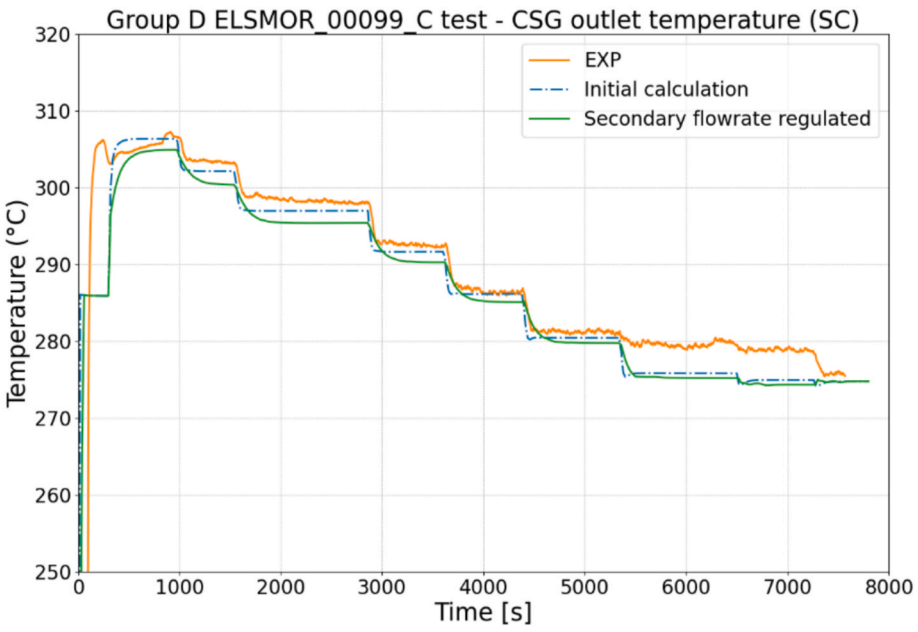

Fig. 12. Group D ELSMOR_00099_C test – CSG outlet temperature (SC) – Initial calculation and calculation with secondary flow rate controlled, compared to experimental data (EXP).

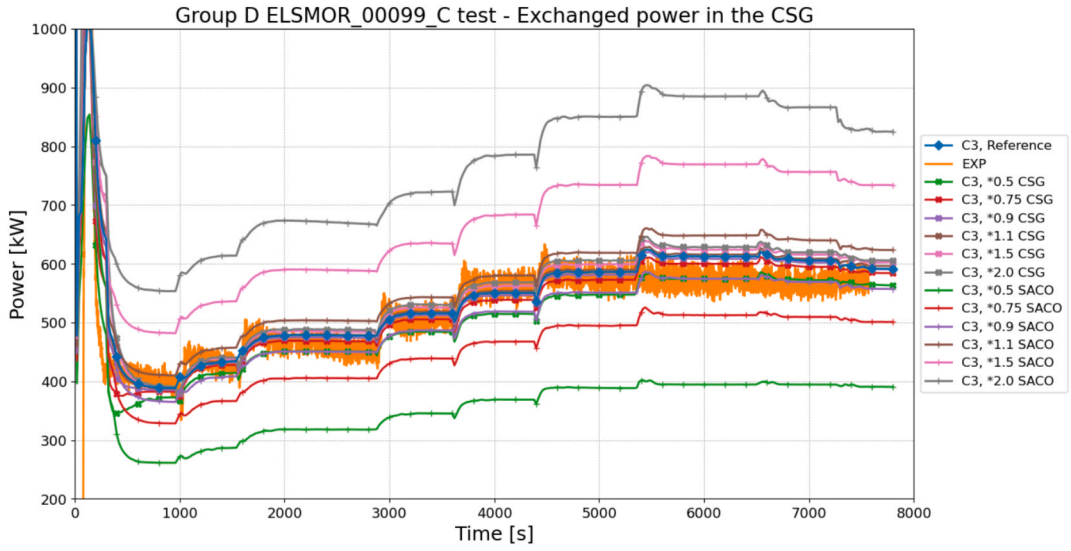

Fig. 13. Group D ELSMOR_00099_C test – Exchanged power in the CSG – Heat exchanger sensitivity calculations on the heat exchanger surface (CSG or SACO) with secondary flow rate controlled, compared to experimental data (EXP). C3 *X EXCH: CATHARE 3 sensitivity calculation with the factor X applied on the heat exchange surface of the heat exchanger EXCH (CSG or SACO).

the PIQUAGE gadget) to match the experimental values according to the time line. The tertiary circuit is not controlled (the temperature and level of the pool evolve freely).

Table 5 presents the initial values of the main loop parameters for both the experimental test and the CATHARE calculation.

The CATHARE 3 results of the initial calculation of this ELSMOR_00099_C test are presented in Figs. 8–12 (the CSG exchanged power, the secondary pressure, the secondary mass flow, the SACO and the CSG outlet temperature in the SC). These results were provided by the CEA for the ELSMOR benchmark (Bersano et al., 2024).

As for the experimental results, the first 400 s of the calculations show large variations (mainly due to the start-up of the system and reaching of steady circulation conditions): this part will not be analysed.

Overall, the CATHARE 3 simulation predicts a good trend, with an increase in power as the FR decreases. This is because, the level in the SACO tubes decreases as the FR decreases, and film condensation (more efficient than liquid convection) becomes increasingly dominant. Similarly, for the pressure and the temperatures in the SC, the qualitative behavior is well predicted by the code.

However, this initial calculation shows significant discrepancies with the experimental results for the secondary flow rate (strong underestimation, see Fig. 10). As explained in section 4, this is due to the fact that no characterisation tests have been carried out on the ELSMOR facility with the secondary side in liquid single-phase (unavailability of a high pressure pump on the secondary side), and therefore the singular head losses have not been included in the modelling. Thus, there are some uncertainties on these head losses, especially on the heat exchangers (CSG and SACO) and the other components (flow meters, valves, etc.).

Due to these uncertainties, and the inaccuracies induced on the secondary flow, it was decided to control this variable. For this purpose,

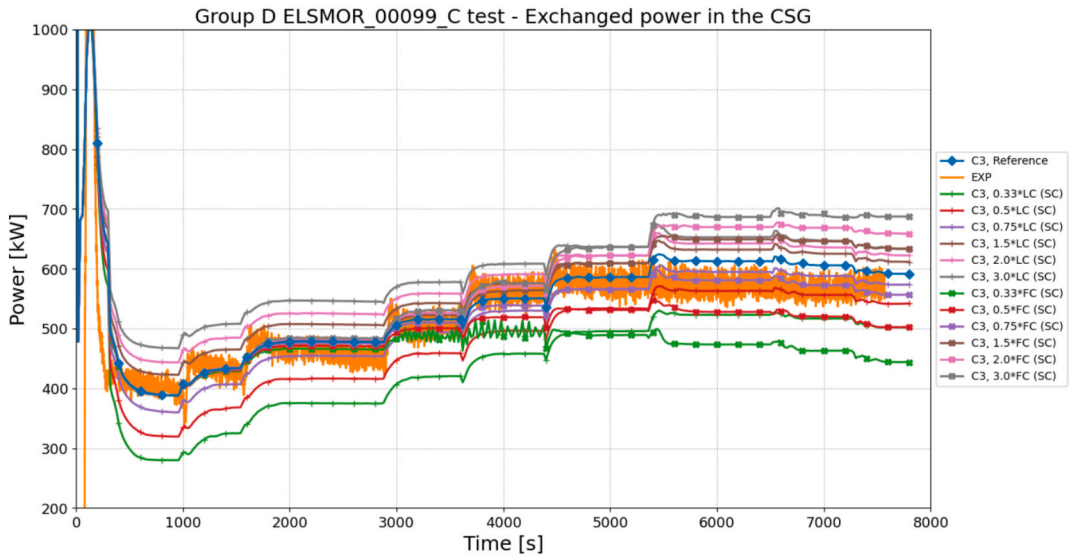

Fig. 14. Group D ELSMOR_00099_C test – Exchanged power on the CSG – Sensitivity calculations on the SACO correlations (secondary side) with secondary flow rate controlled, compared to experimental data (EXP). C3 *X CORR: CATHARE 3 sensitivity calculation with the factor X applied on the CORR correlation (LC for liquid convection, FC for film condensation) on the secondary circuit (SC) of the SACO.

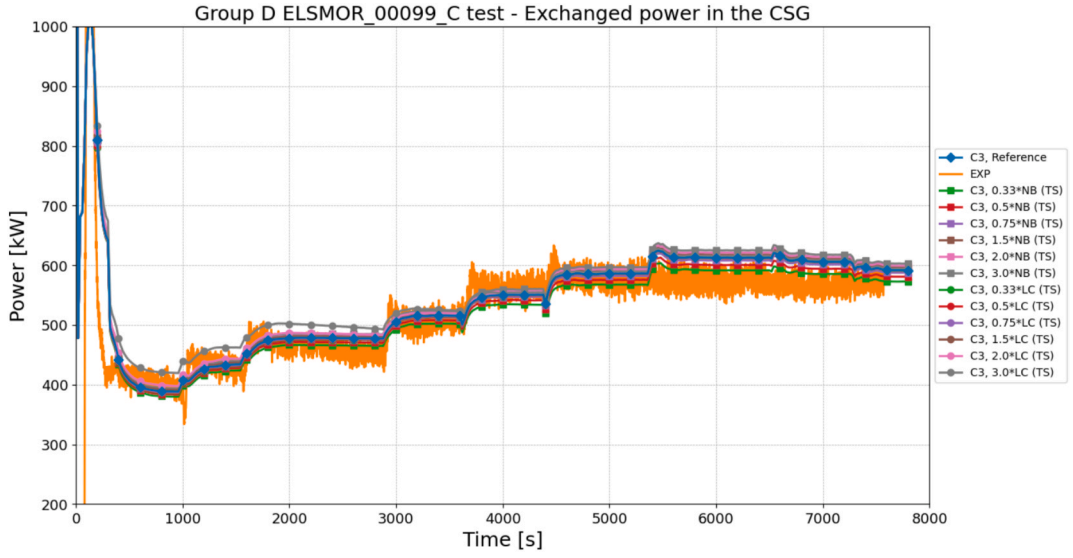

Fig. 15. Group D ELSMOR_00099_C test – Exchanged power on the CSG – Sensitivity calculations on the SACO correlations (tertiary side) with secondary flow rate controlled, compared to experimental data (EXP). C3 *X CORR: CATHARE 3 sensitivity calculation with the factor X applied on the CORR correlation (LC for liquid convection, NB for nucleate boiling) on the tertiary side (TS) of the SACO.

a global head loss (corresponding to a singular head loss) is regulated and added to the cold leg of the secondary circuit in order to adapt the flow rate to the experimental value. At the beginning of the test, the added singular pressure drop coefficient is equal to 25 and is increased throughout the test until it reaches 170 at the end.

Fig. 10 shows this adjustment of the secondary flowrate. The effect of this flow regulation on the power extracted by the CSG is shown in Fig. 8. With this regulation on the secondary flow, the CATHARE 3 code predicts the power exchanged on the CSG satisfactorily (less than 6 % of error with the experimental results (considering the average power value, as it exhibits strong oscillations)) at the beginning of the test (for a higher mass of liquid in the secondary circuit). At the end of the test (for low FR), the discrepancy is higher (about 10 % with the experimental results, still considering the average value) and the CATHARE 3 code overestimates the exchanged power. It tends to prove that the CATHARE 3 code overestimates the film condensation heat transfer in the SACO tubes: this will have to be confirmed in a separate effect test facility, since the current CATHARE 3 validation base (COTURNE facility, (Pilon et al., 1998)) does not cover the fluid Reynolds number (up to 30,000 in ELSMOR, against 2500 in COTURNE) and the heat flux (up to 380 kW/m^2 in ELSMOR, against 60 in COTURNE) encountered in this test.

Moreover, as expected, this increase in the secondary flow rate (compared to the initial calculation) induces an increase in the extracted power: a higher flow rate leads to higher phase velocities in the secondary sides of the exchangers, increasing the heat transfer coefficient. This increase in power extraction is much greater at the beginning of the test, where the discrepancies with the experimental flow are greater.

Despite this regulation of the secondary flow, the secondary pressure is still underestimated by the CATHARE 3 code compared to the experiment. This could be explained by the overestimation of the film condensation in the SACO tubes. The same analysis can be made for the CSG outlet temperature, since the fluid is at saturation; without

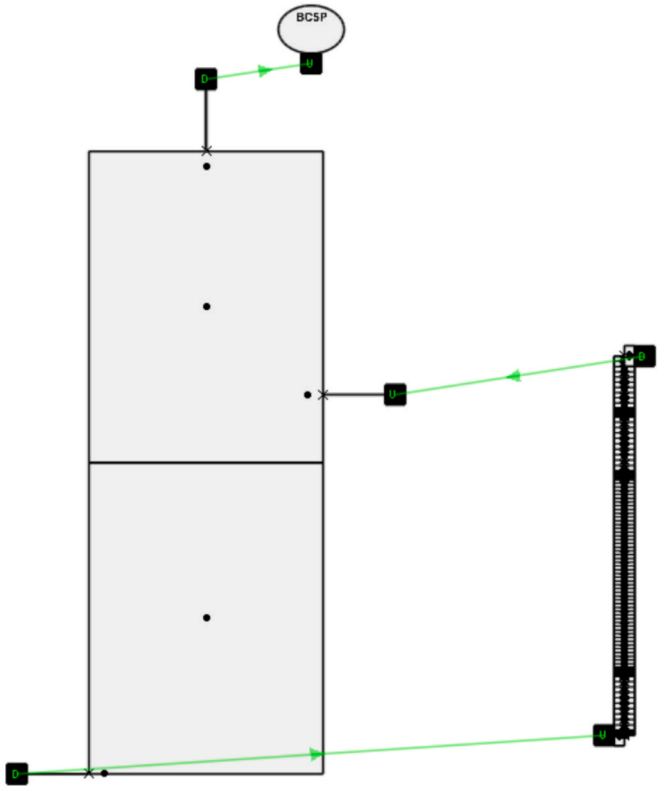

Fig. 16. Alternative modelling for the tertiary circuit.

experimental information on the steam quality, no further analysis can be made.

When the secondary flow is controlled, the SACO outlet temperature in the SC is overestimated at the beginning of the test, but is underestimated at the end. This can be explained by the underestimation (or overestimation) of the extracted power in the CSG (and therefore in the SACO) at the start (or end) of the test.

In order to study this test in depth, it has been decided to determine the most influential correlations for this CATHARE 3 calculation, which can explain the discrepancies with the experimental results, especially on the CSG performance. To this end, the first objective will be to determine which heat exchanger (CSG or SACO) has the greatest impact on the behavior of the loop. Then, if one heat exchanger is identified as the most influential, sensitivity calculations will be performed on its heat transfer correlations to determine which physical phenomena govern its performance.

First, the heat exchange surface of the CSG or SACO is modified (reduced by a factor of 0.9, 0.75 or 0.5, or increased by a factor of 1.1, 1.5 or 2). The effect of these modifications on the CSG performance is shown in Fig. 13 (for these sensitivity calculations, the secondary flow is still controlled).

These results show two main points:

- The SACO is the limiting component for the loop performance (a modification of the thermal surface of this component leads to a significant impact on the extracted power), while the CSG has a limited impact: this is mainly due to the fact that the CSG has a thermal surface 9 times higher than the SACO,
- The monotony can be observed in these sensitivity calculations (up to a factor 0.5 or 2): a decrease/increase in the factor applied to the thermal surface leads to a decrease/increase in the extracted power (within these limits).

Knowing that the SACO is the limiting component, the effect of modifying the correlations involved in this heat exchanger is tested. These correlations are:

- Liquid convection on the secondary side (inside the tubes) (LC SC in the figures),
- Film condensation on the secondary side (inside the tubes) (FC SC in the figures),
- Liquid convection on the tertiary side (around the tubes) (LC TC in the figures),
- Nucleate boiling on the tertiary side (around the tubes) (NB TC in the figures).

This correlation modification is achieved in the CATHARE 3 code by

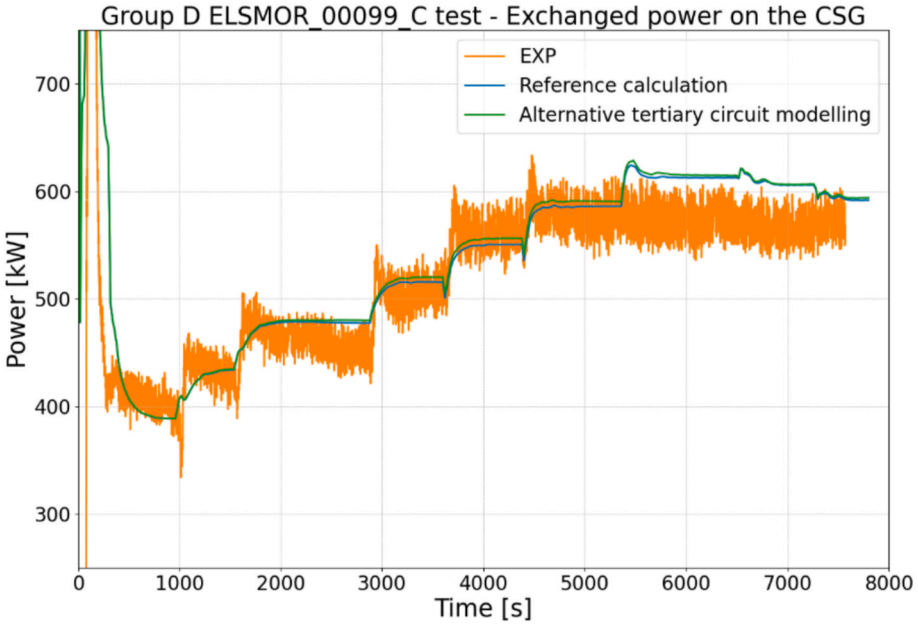

Fig. 17. Group D ELSMOR_00099_C test – Exchanged power in the CSG – Alternative modelling for the tertiary circuit, compared to the reference calculation (with secondary flowrate controlled) and experimental data (EXP).

Table 6
ELSMOR_00090_C_C tests and events timing.

Time (s)	Event	Notes
	Initial filling ratio of the secondary side: 31.20 %Vacuum in the Secondary Side (SS) 0.4 bar.	Valve V_E04 6.5 turns open out of 9.5 turns (fully open)
235	Triggering valve V_E10 opened	Start-up (Triggering valve opening). Vacuum conditions in the SS.
236–679	Natural circulation start-up and stabilization	
680–980	**Steady state at Primary Side (PS) T (TF_082) 310.1 °C; FR 31.20 %**	
1025–1960	PS heat-up transient to 320 °C	
2000–2800	**Steady state at PS T 319.9 °C; FR 31.20 %**	
3105–3187	Injection of non-condensable gas N_2 in SS through V_E06	
3200–3682	**Steady state at PS T 319.4 °C; N_2 70.65 NL; FR 31.20 %**	
3688–3796	Injection of non-condensable gas N_2 in SS through V_E06	
3900–4339	**Steady state at 319.6 °C; N_2 240.97 NL; FR 31.20 %**	
4340–4387	Injection of non-condensable gas N_2 in SS through V_E06	
4500–5114	**Steady state at 320.2 °C; N_2 384.27 NL; FR 31.20 %**	
5115–5228	Injection of non-condensable gas N_2 in SS through V_E06	
5340–5787	**Steady state at 320.4 °C; N_2 536.19 NL; FR 31.20 %**	
5788–5801	Injection of non-condensable gas N_2 in SS through V_E06	
5825–6484	**Steady state at 319.4 °C; N_2 707.58 NL; FR 31.20 %**	
6485–6509	Injection of non-condensable gas N_2 in SS through V_E06	
6521–6999	**Steady state at 319.3 °C; N_2 828.08 NL; FR 31.20 %**	
7000–7116	Injection of non-condensable gas N_2 in SS through V_E06	
7120–7299	**Steady state at 319.6 °C; N_2 950.02 NL; FR 31.20 %**	
7311–7910	Refilling of HX-Pool through V009 by opening FCV07	

Table 7
Experimental and calculation initial value of the test ELSMOR_00090_C_C for the main loop parameters.

Parameter	Experimental initial value	CATHARE initial value
Primary-side CSG inlet temperature	310.5 °C	310 °C
Primary-side CSG inlet flowrate	3.13 kg/s	3 kg/s
Primary-side CSG inlet quality	0	0
SC filling ratio	31.2 %	31.2 %
SC non-condensable mass	Supposed 0 g	0 g
Pool temperature	13.2 °C	13 °C

multiplying the heat transfer coefficient by a factor. For example, for the Dittus-Boelter correlation (Bestion, 1990) used for forced liquid convection (with $f_{convliq}$ the multiplying factor):

$$Nu = 0.023 Re_L^{0.8} Pr_L^{0.4} f_{conv\,liq} \quad (1)$$

with:

- Nu the Nusselt number,
- Re_L the liquid Reynolds number,
- Pr_L the liquid Prandtl number,
- $f_{convliq}$ the multiplying factor.

The effect of these correlation modifications on the CSG performance is shown in Fig. 14 for the secondary side and in Fig. 15 for the tertiary side (for these sensitivity calculations, the secondary flow is still controlled).

First, monotony can be observed in these sensitivity calculations (in the range of the factors applied, from 0.33 to 3).

Then, Fig. 15 shows that the tertiary side correlations (liquid convection and nucleate boiling) have a small influence on the extracted power. Only the secondary side correlations (liquid convection and film condensation) have a significant effect (see Fig. 14).

Fig. 14 also shows that the effect of the secondary side liquid convection modification is higher at the beginning of the test, while the effect of the film condensation modification is higher at the end. This is because, the FR is high (low) at the start (end) of the test, leading to a high (low) water level in the SACO tubes, so that liquid convection (film condensation) is the dominant phenomenon.

Finally, an alternative modelling of the tertiary circuit is tested. Instead of using two AXIAL-elements and two VOLUME-elements as for the reference calculation (see Fig. 7), the tertiary circuit is modelled using only one AXIAL-element for the ascending flow near the HX tube part, and one VOLUME-element for the pool. This alternative modelling is shown in Fig. 16.

The effect of this modelling change on the extracted power is shown in Fig. 17. The reference calculation is the one with the secondary flow regulated (see Fig. 8).

The results show that this change in the modelling of the tertiary circuit has a small effect on the power exchanged in the CSG. This is consistent with the sensitivity calculations carried out on the correlations for the tertiary side of the SACO, where the results showed no significant impact of these correlations on the results (see Fig. 15). The modelling of the tertiary circuit is therefore not an issue for this test, fortunately, as modelling such a component with strong 3D effects can be challenging for a system code using 1D and 0D elements.

5.2. *Test ELSMOR_00090_C_C – Group C*

Table 6 shows the sequence of events for the ELSMOR_00090_C_C test. The main objective of this test is to investigate the effect of NC gas in the SC on the facility behavior, up to 950 Nl of nitrogen. The primary flow rate in the CSG is maintained around 3 kg/s, while the inlet temperature starts at 310 °C and is then increased to 320 °C. The FR in the SC in constant throughout the test, at 31.2 %.

The NC gas is injected into the hot leg of the SC, just before the SACO.

To model this test, the boundary conditions are imposed on the primary side of the CSG. The liquid mass of the secondary circuit is regulated (using the PIQUAGE gadget) to reach the experimental value. The tertiary circuit is not controlled (the temperature and the level of the pool evolve freely). Non-condensable gas is injected into the hot leg of the SC using another PIQUAGE gadget. For the same reason as in the group D test (see section 5.1), the secondary flow is regulated to match the experimental value.

Table 7 presents the initial values of the main loop parameters for both the experimental test and the CATHARE calculation.

The CATHARE 3 results of the calculation on this ELSMOR_00090_C_C test (the CSG exchanged power, the secondary pressure and the SACO outlet temperature in the SC) are presented in Figs. 18–20.

Three sensitivity calculations were also carried out on the injected NC gas mass: a case without NC and two cases with 20 % decrease or increase of the injected mass compared to the reference case.

First of all, we can see the effect of the NC injection in the calculation on the performance of the system. During injection, the power extracted by the loop is greatly reduced: this is due to the gas passing through the SACO tubes. It creates a layer at the liquid–vapor interface, adding a thermal resistance that limits the heat exchange through the film condensation, causing a decrease in power extraction (Fig. 21, left). This phenomenon is modelled in the CATHARE 3 code with the modified

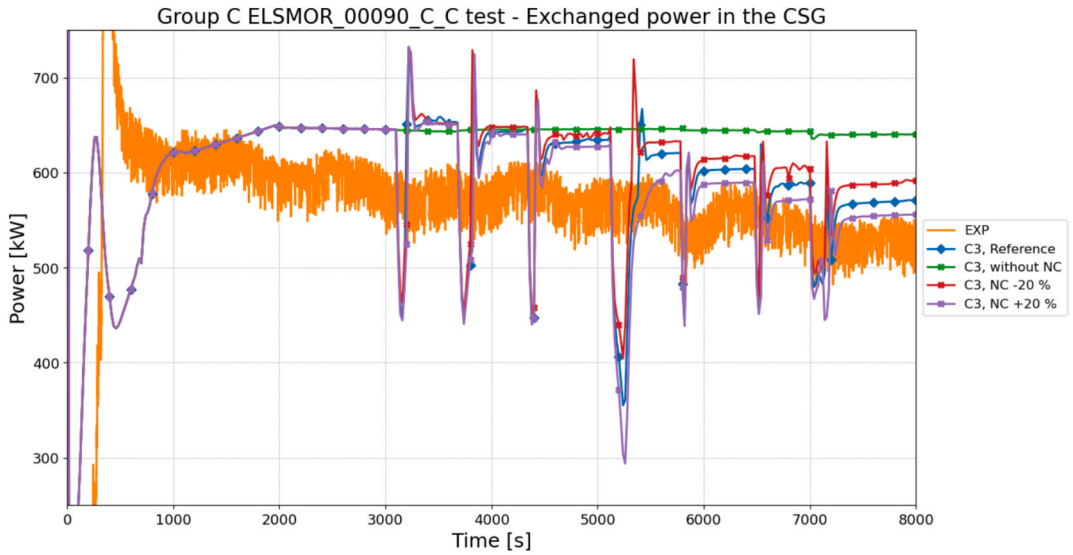

Fig. 18. Group C ELSMOR_00090_C_C test – Exchanged power in the CSG – Reference calculation and sensitivity calculations on the non-condensable gas injected mass (without NC, and NC gas mass with 20 % decrease or increase), compared to experimental data (EXP).

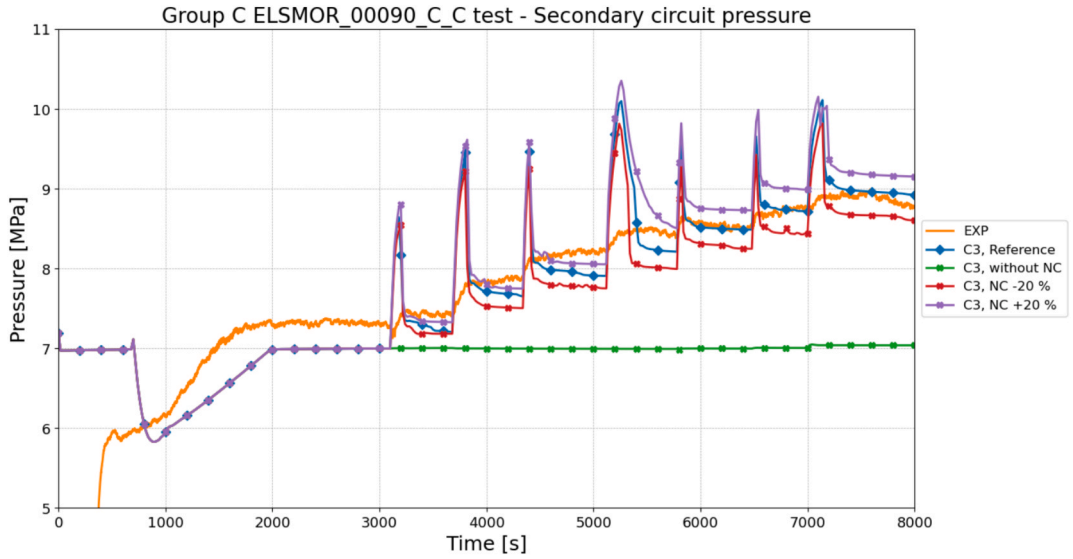

Fig. 19. Group C ELSMOR_00090_C_C test – Secondary circuit pressure – Reference calculation and sensitivity calculations on the non-condensable gas injected mass (without NC, and NC gas mass with 20 % decrease or increase), compared to experimental data (EXP).

Chen correlation, which models film condensation in the presence of NC gases (Bestion et al., 1994; Geffraye et al., 2005). The NC gas gradually accumulates at the end of the film condensation zone, above the level of condensate liquid. This NC gas layer reduces the heat surface available for film condensation, which explains the decrease in power after an injection compared to the power extracted before the injection (Fig. 21, right).

Fig. 22 illustrates this phenomenon in the reference calculation, showing the NC gas mass fraction (MF) and void fraction profiles in the SACO (the SACO tube zone is shown by the black vertical bars, starting at 1.143 m and ending at 3.245 m):

- Before the 4th injection (5100 s), the NC gas is located at the bottom of the tubes (NC gas presence starts at 2.57 m); upstream, the two-phase flow is pure, there is no NC gas,
- During the 4th injection (5150 s), a NC gas profile is observed in the SACO tubes (the two-phase flow is not pure, it is mixed with nitrogen),
- After the 4th injection (5600 s), the injected NC gas accumulated at the bottom of the tubes, increasing the height of NC gas layer (NC gas presence now starts at 2.43 m, against 2.57 m before the injection); upstream, the flow returns to a pure two-phase flow, without NC.

This behavior in the SACO tubes during the injection phases is not observed in the experimental results. This can be explained by the dimension of the tubes: most of the NC gas can be in the centre of the flow, slightly disturbing the condensation at the interface.

Despite this phenomenon during the injection phases, the CATHARE 3 simulation predicts the good tendency compared to the experimental results during this test, with a power decrease after each injection (explained by the NC gas accumulation in the SACO tubes, see above), leading to an increase of the SC pressure. The decrease in SACO outlet temperature after each injection is also well predicted by the simulation.

Before the first injection, the reference calculation overestimates the exchanged power (about 8 %), which is consistent with the equivalent point in the Group D test (between 5630 and 6400 s, see Fig. 8). This

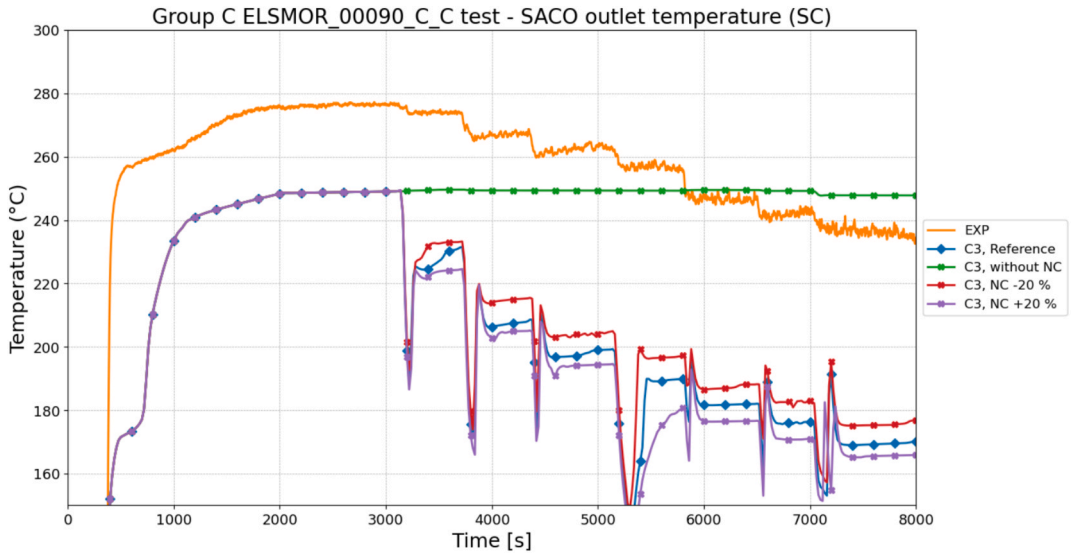

Fig. 20. Group C ELSMOR_00090_C_C test – SACO outlet temperature (SC) – Reference calculation and sensitivity calculations on the non-condensable gas injected mass (without NC, and NC gas mass with 20 % decrease or increase), compared to experimental data (EXP).

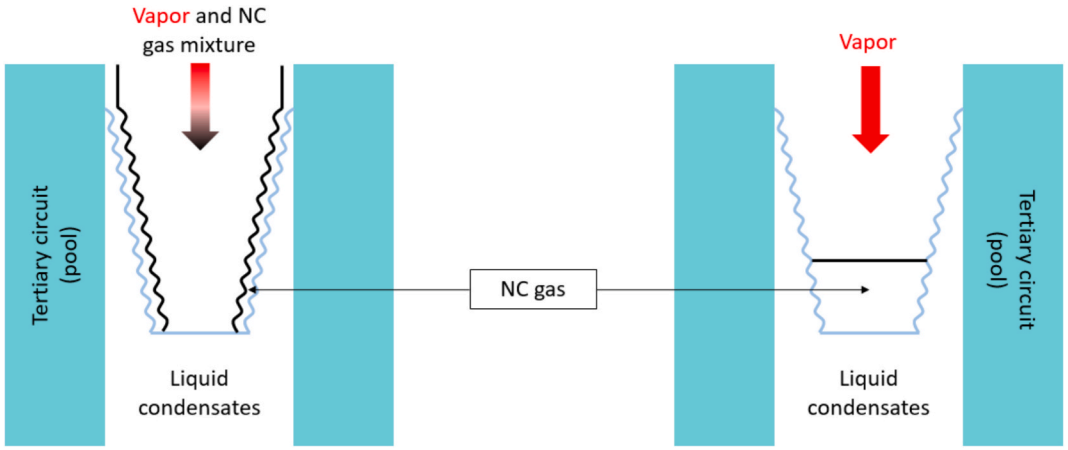

Fig. 21. Schematic representation of the behavior of the NC gas in the SACO tubes and influence on the film condensation during the injection (left) and after the injection (right).

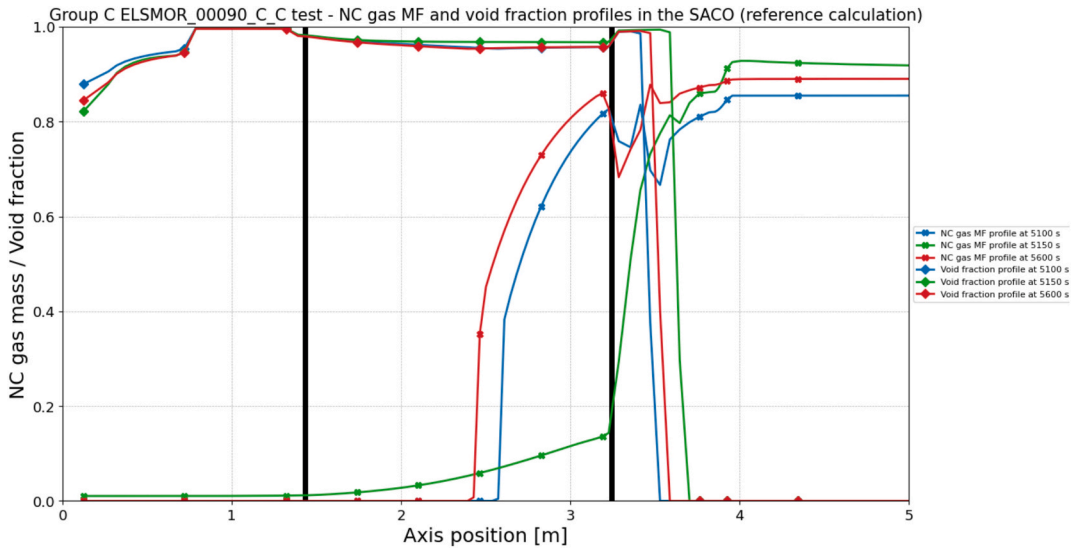

Fig. 22. Group C ELSMOR_00090_C_C test – NC gas MF and void fraction profiles in the SACO – Reference calculation.

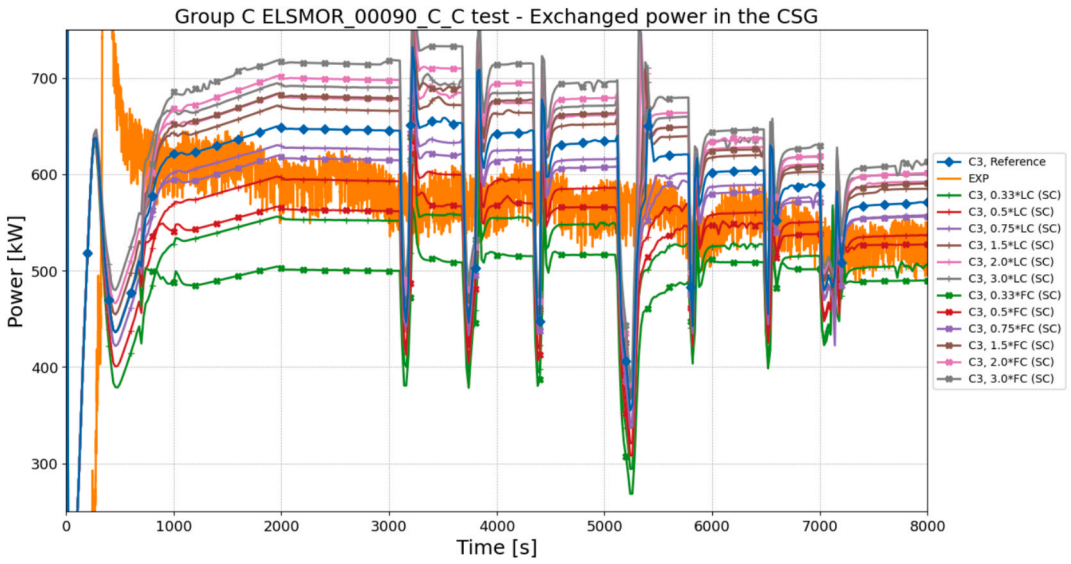

Fig. 23. Group C ELSMOR_00090_C_C test – Exchanged power in the CSG – Sensitivity calculations on the SACO correlations (secondary side), compared to experimental data (EXP). C3 *X CORR: CATHARE 3 sensitivity calculation with the factor X applied on the CORR correlation (LC for liquid convection, FC for film condensation) on the secondary circuit (SC) of the SACO.

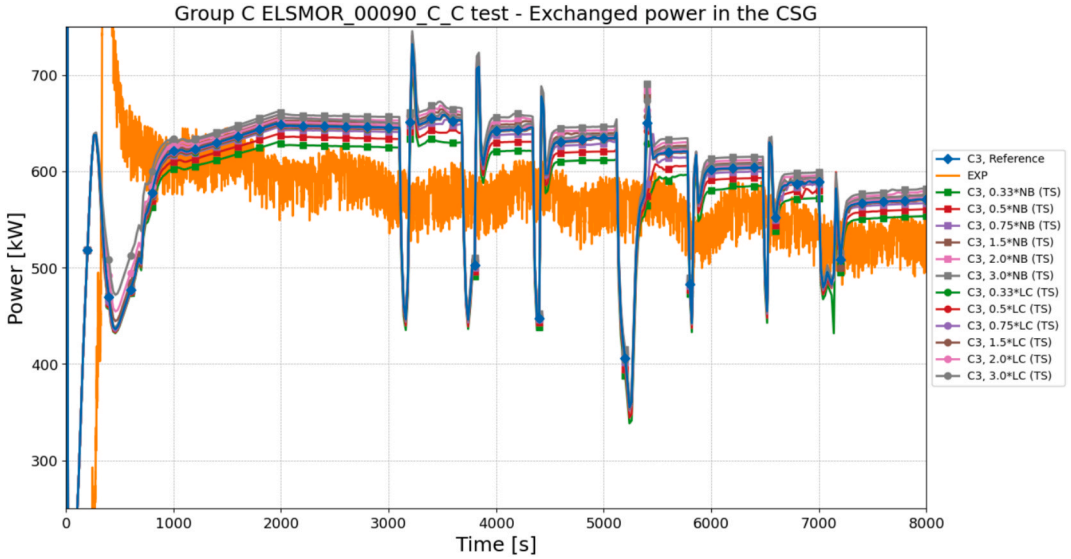

Fig. 24. Group C ELSMOR_00090_C_C test – Exchanged power in the CSG – Sensitivity calculations on the SACO correlations (tertiary side), compared to experimental data (EXP). C3 *X CORR: CATHARE 3 sensitivity calculation with the factor X applied on the CORR correlation (LC for liquid convection, NB for nucleate boiling) on the tertiary side (TS) of the SACO.

overestimation of the exchanged power remains globally identical throughout the test, with NC gas injections.

The sensitivity calculations on the injected NC gas mass allow to measure the influence of the NC on the film condensation and thus on the extracted power. The extracted power with 950 Nl of N_2 (corresponding to 1.1 kg) is reduced by 70 kW (about 11 %) compared to the case without NC. A change of 20 % in the injected NC gas mass can change the extracted power predicted by the code by up to 3.5 %.

In addition, similarly to group D, sensitivity calculations were performed on the correlations involved in the SACO (film condensation, nucleate boiling, and film condensation on both sides), see Figure 23 and Figure 24.

The results of these sensitivity calculations are similar to those obtained for the equivalent FR in the Group D test:

- Film condensation has the largest effect on the loop performance (due to the relatively low FR),
- Liquid convection on the secondary side also has a significant effect,
- The tertiary correlations have a limited effect on the loop performance (and therefore on the tertiary circuit modelling).

5.3. *Test ELSMOR_00134_C – Group F*

Table 8 shows the timing of events for the ELSMOR_00134_C test. The main objective of this test is to investigate the behavior of the facility with a two-phase flow in the primary side of the CSG. The primary flowrate is approximately 0.5 kg/s, while the CSG inlet temperature is maintained at 310 °C. The FR starts at 39.2 %, and is then reduced to 20 %.

To model this test, the boundary conditions are imposed on the primary side of the CSG. The secondary circuit liquid mass is controlled

Table 8
ELSMOR_00134_C tests and events timing.

Time (s)	Event	Notes
	Initial filling ratio of the secondary side: 39.2 %Vacuum in the Secondary Side (SS) 0.5 bar.	Valve V_E04 9.5 turns open (fully open)Orifice F_1001 d = 89.9 mm (smaller orifide installed)
143	Triggering valve V_E010 opened	Test started with PS flowrate ~22 kg/s and Separator level ~3.4 m (CSG lower connection from separator bottom)
135–1830	Natural circulation start-up. Separator level increase due fluid flashing for too high pressure drops of two-phase flow in the 4-inch pipe between EH101 and Separator inlet (145–780 s). PS flowrate reduced by operator to limit pressure drops until Separator level goes to ~3.4 m (577–780 s). Separator level stabilization below 3.4 m	
1850–2445	**Steady state at Primary Side (PS) T (TF_082) 310.15 °C; FR 39.2; SS P 8.85 MPa**	
2447–2555	11.3 kg extracted from the SS, FR = 30.16 %	
2690–3050	**Steady state at PS T 309.82 °C; FR 30.16; SS P 7.32 MPa**	
3200–3500	**Steady state at PS T 310.08 °C; FR 30.16; SS P 8.36 MPa**	
3438–3488	12.7 kg extracted from the SS, FR = 20.00 %	
3800–3975	**Steady state at PS T 309.72 °C; FR 20.00 %; SS P 6.52 MPa**	
4000–4297	**Steady state at PS T 309.36 °C; FR 20.00 %; SS P 7.09 MPa**	
4297	End of test	

Table 9
Experimental and calculation initial values of the test ELSMOR_00134_C for the main loop parameters.

Parameter	Experimental initial value	CATHARE initial value
Primary-side CSG inlet temperature	310.3 °C	310 °C
Primary-side CSG inlet flowrate	0.52 kg/s	0.5 kg/s
Primary-side CSG inlet quality	Supposed 1	Depends on the calculation performed
SC filling ratio	39.2 %	39.2 %
SC non-condensable mass	Supposed 0 g	0 g
Pool temperature	8.8 °C	10 °C

(using the PIQUAGE gadget) to match the experimental values according to the timeline. The tertiary circuit is not controlled (the temperature and the level of the pool evolve freely). For the same reason as in the group D test (see section 5.1), the secondary flow is controlled to match the experimental value.

Table 9 presents the initial values of the main loop parameters for both the experimental test and the CATHARE calculation.

Because there is an experimental uncertainty on this parameter, four calculations with different CSG inlet flow quality are tested: pure steam ($\alpha_{inlet} = 1$), two-phase flow ($\alpha_{inlet} = 0.9$ and $\alpha_{inlet} = 0.5$) and pure liquid ($\alpha_{inlet} = 0$). The purpose of these sensitivity calculations is to study the impact of this boundary condition on the loop behavior.

The experimental and the calculated results for the exchanged power in the CSG, the secondary circuit pressure and the SACO outlet temperature in the SC are shown in Fig. 25, Fig. 26, and Fig. 27, respectively.

The main difficulty in this test is the estimation the experimental exchanged power. In fact, for the other tests (from the group C or D, see 5.1 and 5.2), the extracted power was calculated with a power balance on the primary side of the CSG:

$$P_w = Q_{in,CSG}.C_p.(T_{in,CSG} - T_{out,CSG}) \quad (2)$$

with:

- P_W the exchanged power,
- $Q_{in,CSG}$ the mass flowrate at the inlet of the CSG on the primary side,
- C_p the heat capacity,
- $T_{in,CSG}$ and $T_{out,CSG}$ respectively the inlet and outlet temperature of the CSG on the primary side.

This was relevant in the previous tests, because the flow at the CSG inlet was pure liquid, but not here for Group F, due to the two-phase flow. This estimated power (labelled "W_CSG_PS" in Fig. 25) is then underestimated.

For a better estimation of the exchanged power, the latent heat contribution should be taken into account:

$$P_w = Q_{in,CSG}.C_p.\left(T_{in,CSG} - T_{out,CSG}\right) + Q_{in,CSG}.L \quad (3)$$

with L the latent heat.

This estimated power for the latent heat contribution experiment is labelled "W_CSG_PS_latent" in Fig. 25. The problem with this method is the assumption that the inlet flow is pure steam, but there is no quality measurement at the CSG inlet to verify this.

The same latent heat estimation can be done on the secondary side of the CSG: this estimated power for the latent heat contribution experiment is labelled "W_CSG_SS_latent" in Fig. 25. This estimate suffers from the same uncertainty regarding the quality at the CSG outlet in the SC (no measurement). The fact that this power is greater than the estimated power in the PC tends to prove that this power is overestimated, and that the assumption that the flow at the CSG outlet in the SS is pure steam is probably wrong (it must be a two-phase flow).

The last possibility to estimate the extracted power is to use the pool temperatures and level evolution, shown in Fig. 28 and Fig. 29. Sensors TF_001, TF_020 and TF_040 are placed in the pool at levels corresponding to respectively to the bottom, middle and top of the HX. Sensor TF_060 is located in the upper part of the pool (approximately 70 cm below the water level at the start of the test).

The extracted power can then be estimated using three methods.

The first is to make a power balance on the pool for the whole test:

$$P_w = \frac{m_{pool,init}.C_p.\left(T_{pool,final} - T_{pool,init}\right) + \left(m_{pool,init} - m_{pool,final}\right).L}{t_{test}} \quad (4)$$

with:

- $T_{pool,init}$ and $T_{pool,final}$ respectively the pool temperature at the beginning and the end of the test,
- $m_{pool,init}$ and $m_{pool,final}$ respectively the mass of liquid water at in the pool at the beginning and the end of the test,
- t_{test} the time duration of the test.

The estimated power with this first method is 701.5 kW (solid black line labelled "Global pool" in Fig. 25). The problem with this method is that it does not take into account the heat losses of the loop and the energy required to heat the structures, so it probably underestimates the power exchanged. In addition, it only gives an average value for the whole test and not a temporal evolution.

The second method is to take into account the temperature rise at the beginning of the test (i.e. the gradient between 200 and 2000 s, about 0.05 °C/s, see Fig. 28):

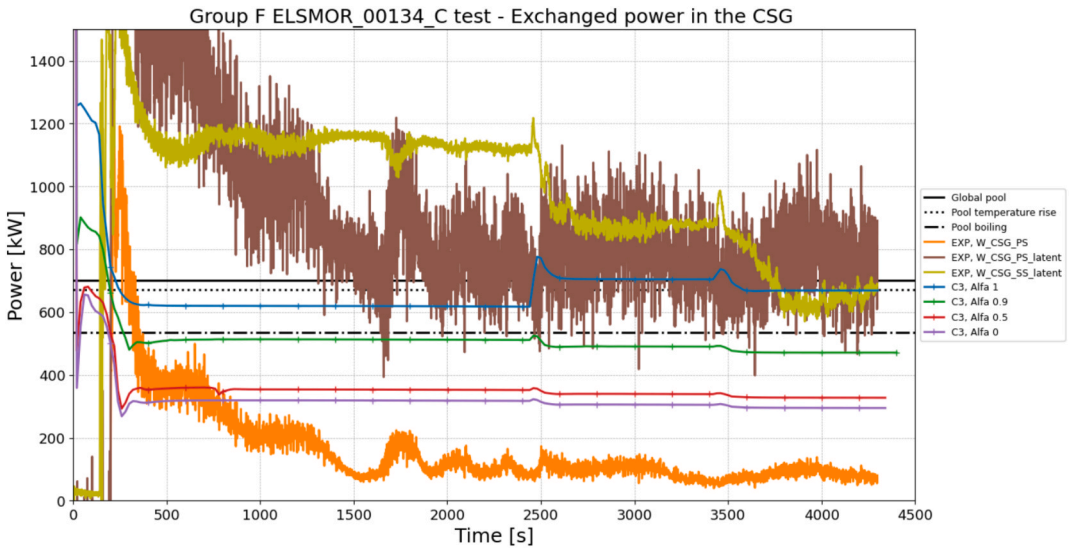

Fig. 25. Group F ELSMOR_00134_C test – Exchanged power in the CSG – Experimental and calculated results. Global pool: experimental estimate with power balance on the pool for the whole test (see (4)); Pool temperature rise: experimental estimate with pool temperature rise at the beginning of the test (see (5)); Pool boiling: experimental estimate with pool boiling at the end of the test (see (6)); EXP, W_CSG_PS(_latent): experimental estimate with a power balance on the primary side (PS) or secondary side (SS) of the CSG, with or without the latent heat contribution (see (2)(3)); C3 Alfa X: CATHARE 3 calculation with the void fraction at the inlet of the CSG set to X.

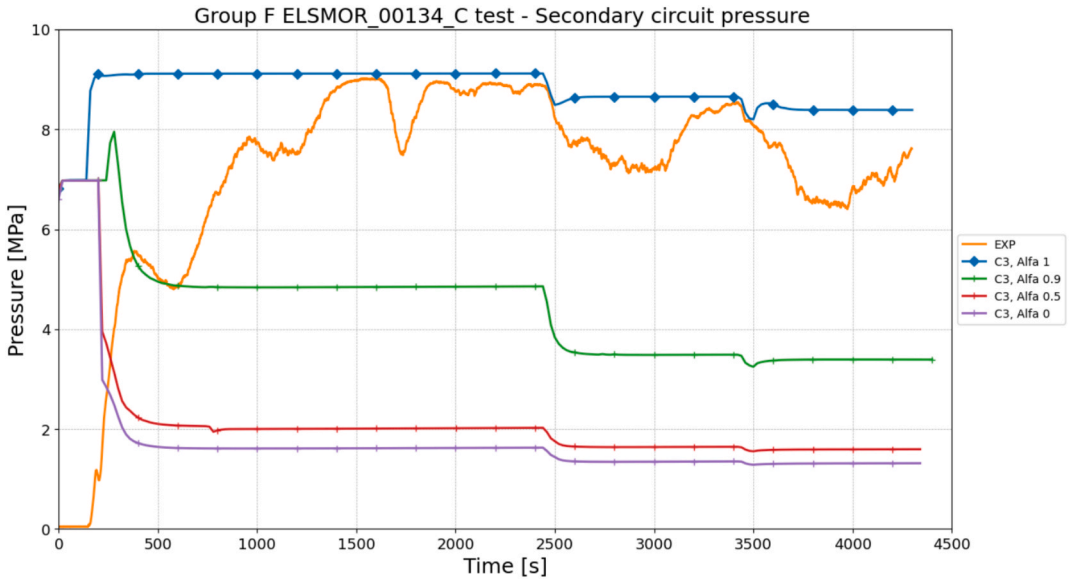

Fig. 26. Group F ELSMOR_00134_C test – Secondary circuit pressure – Experimental (EXP) and calculated results (C3 Alfa X: CATHARE 3 calculation with the void fraction at the inlet of the CSG set to X).

$$P_W = \theta.Cp.m_{pool,init} \tag{5}$$

with θ the gradient of the liquid temperature rise in the pool between 200 and 2000 s in the test.

As the bottom of the pool is not heated at the start of the test (see TF_001 temperature), it is not included in the water mass of the pool. The estimated power using this second method is 672.5 kW (dotted black line labelled "Pool temperature rise" in Fig. 25). The problem with this method is also that it does not take into account the heat losses of the circuit and the energy required to heat the structures, and therefore it probably underestimates the power exchanged. Furthermore, this estimated power is only relevant for the beginning of the test (t < 2000 s).

The third and last method is to consider the boiling of the pool, when all the water is saturated (including the bottom of the pool, see TF_001 in the Fig. 28): this corresponds to the end of the test (for t > 3500 s, see Fig. 29).

$$P_W = \frac{m_{evap}.L}{t_{boiling}} \tag{6}$$

with:

- m_{evap} the mass of liquid evaporated in the pool between 3500 s and the end of the test,
- $t_{boiling}$ the time duration between 3500 s and the end of the test.

The estimated power using this third method is 536.5 kW (dashed black line labelled "Pool boiling" in Fig. 25). The problem with this method is also that it does not take into account the heat losses of the

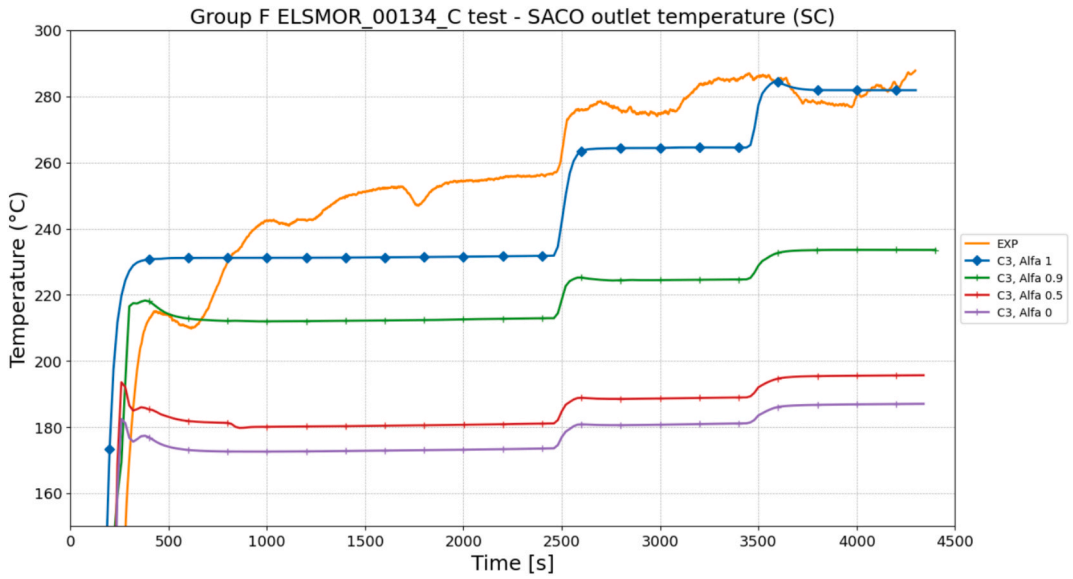

Fig. 27. Group F ELSMOR_00134_C test – SACO outlet temperature (SC) – Experimental (EXP) and calculated results (C3 Alfa X: CATHARE 3 calculation with the void fraction at the inlet of the CSG set to X).

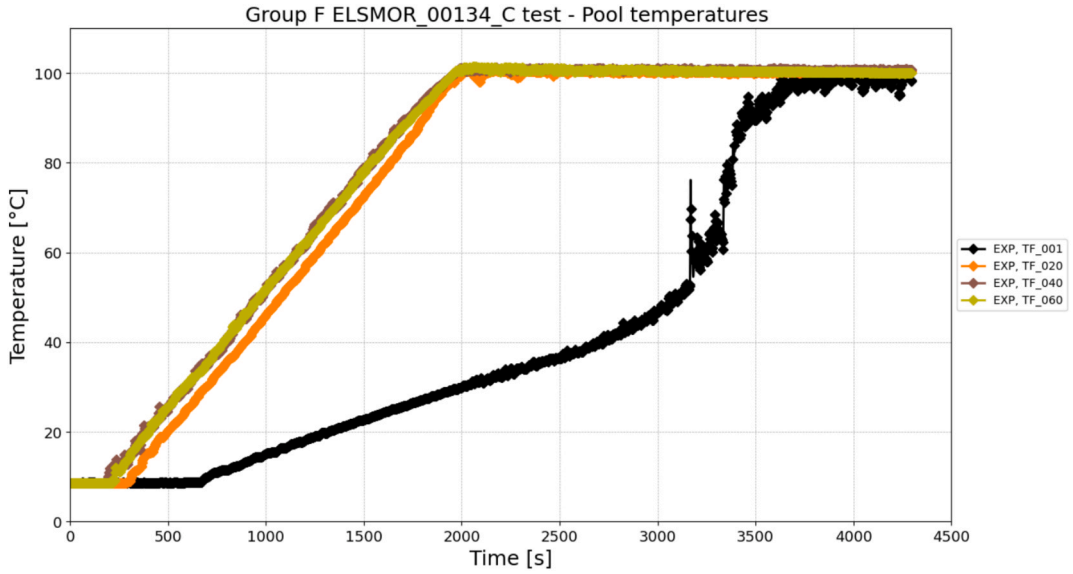

Fig. 28. Group F ELSMOR_00134_C test – Pool temperatures– Experimental results.

loop, and therefore probably underestimates the exchanged power. Furthermore, this estimated power is only relevant for the end of the test ($t > 3500$ s).

With all these methods, it is possible to better estimate the experimental exchange rate. Firstly, it is not relevant to try to estimate it before 1830 s (primary conditions are not stabilised, see Table 8). Moreover, the latent heat should be taken into account in the heat balance of the CSG: the estimated power in the CSG without the latent heat contribution (labelled "W_CSG_PS" in Fig. 25) is significantly lower than the power estimated with the different methods in the pool. As explained earlier, the estimated power in the SS of the CSG (labelled "W_CSG_SS_latent" in Fig. 25) is not relevant and should not be considered, as it is greater than the estimated power at the PS for most of the tests. When the primary conditions are stabilised ($t > 1830$ s), the estimated power in the CSG with the latent heat contribution (labelled "W_CSG_PS_latent" in Fig. 25) is consistent with two of the three methods used to estimate power in the pool. From all these considerations, the estimated power at the PS of the CSG with the latent heat contribution appears to be relevant.

The steam quality at the CSG inlet to the PS has a strong influence on the exchanged power in the CATHARE 3 calculations: the extracted power is twice higher with pure steam than with pure liquid. This can be explained by the higher heat transfer coefficient and the higher temperature difference with the SS in the case of pure steam. In this case, the first decrease of FR (from 39.2 to 30.16 %) increases the exchanged power, while it slightly decreases it in the case of pure liquid. The changes of the FR do not seem to modify the exchanged power in the experiment, but it can be related to the uncertainty of power estimation.

Even in the case of pure steam, the CATHARE 3 calculation seems to underestimate the experimental exchange capacity (estimated in the CSG with the latent heat contribution): about 20 % for the first part of the test (39.2 % of FR), 9 % at 30.16 % of FR, and 14 % at the end of the test (20 % of FR). This is not consistent with the equivalent points in the Group D test, where the CATHARE 3 predicted well or overestimated the

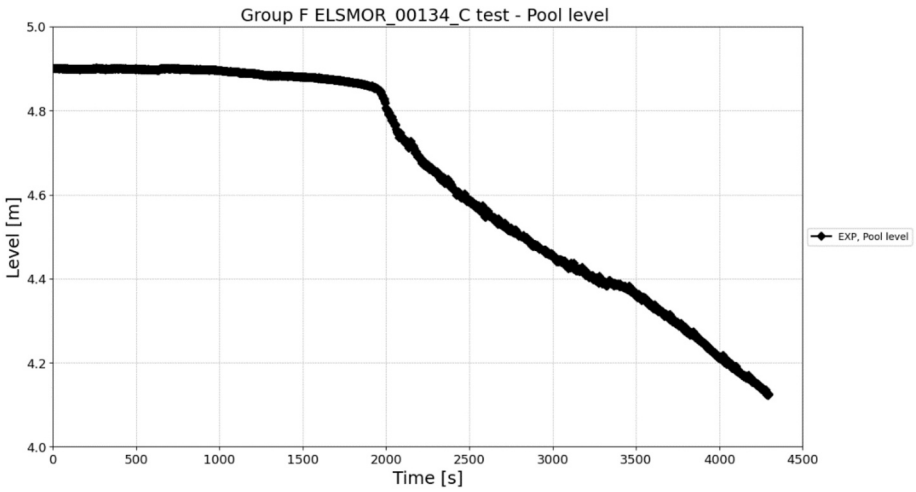

Fig. 29. Group F ELSMOR_00134_C test – Pool level – Experimental result.

experimental exchange capacity: this could be explained by the fact that the CSG plays an important role in this test (unlike in the other tests), and the two-phase exchanges in the primary side of the CSG could be underestimated by the CATHARE 3 code. This analysis should be tempered by the uncertainty associated with the experimental results.

The SACO outlet temperature in the SC is underestimated by the calculation, which is consistent with the other tests.

6. Conclusions

The ELSMOR project, which ended in August 2023, was dedicated to addressing some aspects of LW SMR licensing in Europe through experimental and analytical activities. Within the project, an experimental facility was designed and constructed at SIET to investigate the behavior of a passive heat removal system. A plate-type steam generator (CSG) is used as the heat source of a natural circulation system, while the heat sink is a vertical tube bundle heat exchanger (SACO) immersed in a pool.

Three tests carried out on the facility were then selected and modelled with the CATHARE 3 code:

- Test ELSMOR_00099_C, chosen for the benchmark carried out during the ELSMOR project, to study the influence of the FR in the SC on the behavior of the facility,
- Test ELSMOR_00090_C_C, investigating the impact of the presence of non-condensable gas in the SC on the behavior of the facility,
- Test ELSMOR_00134_C, investigating the behavior of the facility with two-phase flow on the primary side of the CSG.

Due to the fact that no characterisation tests have been performed on the ELSMOR facility, the singular head losses have not been included in the modelling. Therefore, there are some uncertainties on these head losses: it was decided to adjust the secondary circuit flow rate in the calculations to match the experimental values.

These CATHARE 3 calculations showed that:

- The CATHARE 3 code predicts good trends for the tests: decrease of the exchanged power in the CSG and increase of the SC pressure with the decrease of the FR or the increase of the NC gas mass in the SC,
- The error of the CATHARE 3 code compared to the experimental results for the exchanged power in the CSG is less than 10 % for the tests ELSMOR_00099_C and ELSMOR_00090_C_C; this error goes up to 20 % for the test ELSMOR_00134_C, but the uncertainty on the experimental power is higher (due to the two-phase flow on the primary side of the CSG),
- For high FR in the SC, the CATHARE 3 code tends to predict the exchanged power well (with a slight underestimation), while for low FR the power is overestimated,
- Sensitivity calculations showed that the SACO has the main influence on the facility behavior (the CSG has a limited influence); in particular, the SS correlations in the SACO (liquid convection and film condensation) have a significant influence on the exchanged power, while the tertiary side correlations (liquid convection and nucleate boiling) have a small influence; thus, the tertiary modelling has a small influence on the calculation results,
- For all tests, the CATHARE 3 code underestimates the SACO outlet temperature and overestimates the pressure in the SC,
- These observations tend to prove that the CATHARE 3 code overestimates the film condensation heat transfer in the SACO tubes (but this needs to be confirmed in a separate effect test facility).

This work could be completed with the presentation of the calculations performed on the other tests on the ELSMOR facility. Future work on separate effect test facilities may also provide additional data on the film condensation phenomenon in the SACO tubes for the thermohydraulic conditions encountered in the ELSMOR tests, and confirm the overestimation of the heat transfer with the current CATHARE 3 model.

CRediT authorship contribution statement

B. Grosjean: Writing – review & editing, Writing – original draft. **R. Ferri:** Validation. **C. Lombardo:** Validation.

Declaration of competing interest

The authors declare that they have no known competing financial interests or personal relationships that could have appeared to influence the work reported in this paper.

Acknowledgements

The authors wish to thank J. Martin for his participation in the CATHARE modelling of the ELSMOR facility, and C. Capieu for his participation in the CATHARE calculations performed on the tests.

Data availability

Data will be made available on request.

References

Achilli, A., Cattadori, G., Ferri, R., Rigamonti, M., Bianchi, F., Meloni, P., 2002. PERSEO project: experimental facility set-up and RELAP5 code calculation. Presented at the 40th European Two-Phase Flow Group Meetings, Stockholm.

Bae, B.-U., Yun, B.-J., Kim, S., Kang, K.H., 2012. Design of condensation heat exchanger for the PAFS (Passive Auxiliary Feedwater System) of APR+ (Advanced Power Reactor Plus). Ann. Nucl. Energy 46, 134–143. https://doi.org/10.1016/j.anucene.2012.03.029.

Bakhmet'ev, A.M., Bol'shukhin, M.A., Vakhrushev, V.V., Khizbullin, A.M., Makarov, O. V., Bezlepkin, V.V., Semashko, S.E., Ivkov, I.M., 2009. Experimental validation of the cooling loop for a passive system for removing heat from the AES-2006 protective envelope design for the Leningradskaya nuclear power plant site. At. Energ. 106, 185–190. https://doi.org/10.1007/s10512-009-9150-1.

Bersano, A., Lombardo, C., 2022. Test specification and pretest analysis results for natural circulation with prototypical heat exchanger. ELSMOR.

Bersano, A., Lombardo, C., Alblouwy, F., Karppinen, I., Silde, A., Nikitin, K., Grosjean, B., Morin, F., Martin, J., Weyermann, F., 2024. Benchmark exercise on ELSMOR passive heat removal system. Nucl. Eng. Des. 419, 112961. https://doi.org/10.1016/j.nucengdes.2024.112961.

Bestion, D., 1990. The physical closure laws in the CATHARE code. Nucl. Eng. Des. 124, 229–245. https://doi.org/10.1016/0029-5493(90)90294-8.

Bestion, D., Coste, P., Barsotti, S., 1994. Study on condensation modeling in the Cathare code with and without non condensible gas. Presented at the New trends in Nuclear System Thermohydraulics, Pise.

Ferri, Achilli, A., Congiu, C., Marcianò, S., Gandolfi, S., Marengoni, M., Bersani, A., Passerin D'Entreves, A., 2023a. ELSMOR European project: experimental results on an innovative decay heat removal system based on a plate-type heat exchanger. Sci. Technol. Nucl. Install. 2023, 6672504. https://doi.org/10.1155/2023/6672504.

Ferri, Congiu, C., Achilli, A., Gandolfi, S., Marcianò, S., Marengoni, M., Bersano, A., 2023b. ELSMOR D3.4: Test report for natural circulation with prototypical heat exchanger. ELSMOR.

Francis, D., Beils, S., 2024. NUWARD SMR safety approach and licensing objectives for international deployment. Nucl. Eng. Technol. 56, 1029–1036. https://doi.org/10.1016/j.net.2023.12.045.

Geffraye, G., Bestion, D., Kalitvianski, V., 2005. Modelling of film condensation in presence of non condensable gases.

Gómez-García-Toraño, I., Schollenberger, S., Dennhardt, L., Wielenberg, A., Vernassière, M., Buchholz, S., Al-Yahia, O.S., Garcia, E., Polidori, M., Sobecki, N., Lahovský, F., de-Bouet-du-Portal, F., Grippo, G., Montout, M., 2025. Experimental and numerical analysis on safety condenser performance based on P1 experiments at the PKL facility. Nucl. Eng. Des. 438, 114016. https://doi.org/10.1016/j.nucengdes.2025.114016.

Idelchik, I.E., 2008. Handbook of Hydraulic Resistance, 4th Edition Revised and Augmented. Begell House Inc. doi: 10.1615/978-1-56700-251-5.0.

International Atomic Energy Agency, 2020. Advances in Small Modular Reactor Technology Developments (IAEA Advanced Reactor Information System (ARIS)). International Atomic Energy Agency, Vienna.

Montout, M., Herer, C., Telkkä, J., 2024. PASTELS project - overall progress of the project on experimental and numerical activities on passive safety systems. Nucl. Eng. Technol. 56, 803–811. https://doi.org/10.1016/j.net.2023.08.021.

NEA-OECD, 2024. Status Report on Reliability of Thermal-Hydraulic Passive Systems. OECD Nuclear Energy Agency, Paris.

Pilon, L., Geffraye, G., Chataing, T., 1998. Validation of the CATHARE film condensation model on COTURNE experiment. Presented at the 6th Int. Conf. on Nuclear Engineering, San Diego.

Préa, R., Fillion, P., Matteo, L., Mauger, G., Mekkas, A., 2020. CATHARE-3 V2.1: The new industrial version of the CATHARE code. Presented at the ATH'20 - Advances in Thermal Hydraulics 2020, p. https://www.ans.org/pubs/proceedings/article.

Schaffrath, A., Hicken, E.F., Jaegers, H., Prasser, H.-M., 1999. Operation conditions of the emergency condenser of the SWR1000. Nucl. Eng. Des. 188, 303–318. https://doi.org/10.1016/S0029-5493(99)00044-8.

Vernassière, M., 2022. Validation de CATHARE-3 pour un SACO vertical basée sur les essais PKL-ETHARINUS J4.1.

Xing, J., Song, D., Wu, Y., 2016. HPR1000: advanced pressurized water reactor with active and passive safety. Engineering 2, 79–87. https://doi.org/10.1016/J.ENG.2016.01.017.

Zhang, Y.P., Qiu, S.Z., Su, G.H., Tian, W.X., 2012. Design and transient analyses of emergency passive residual heat removal system of CPR1000. Nucl. Eng. Des. 242, 247–256. https://doi.org/10.1016/j.nucengdes.2011.09.036.